

On-Wafer Load-Pull for Millimeter-Wave Applications Above 100GHz

by

Louis Lukaczyk

A thesis submitted in partial fulfillment of the requirements for the degree of

Master of Science

Department of Electrical and Computer Engineering
University of Virginia

© Louis Lukaczyk, 2019

Acknowledgements

Thank you to members of FIR and cleanroom staff for ideas, support, and training

Table of Contents

1	Introduction	1
1.1	Load Pull Background	2
1.2	Selection of Tunable Elements for Millimeter Wave Load Pull device	4
2	WR-5.1 Waveguide E-H Tuner	6
2.1	Waveguide E-H Junction Construction	6
2.2	Waveguide Non-contact Sliding Short	8
2.3	E-H Tuner Measurements	11
2.4	E-H Tuner Simulated Network Cascade with Probe	16
3	Double Slug MEMS Tuner for On-wafer Load Pull Probe	18
3.1	Double Slug MEMS Device Simulations	20
3.2	Double Slug Tuner Theory	20
3.3	Design of WR-5.1 MEMS Double Slug Tuner on Silicon membrane	22
3.4	Proposed Geometry and Fabrication of WR-5.1 Double Slug Tuner Test structure and On-Wafer Probe	30
4	Conclusions, Recommendations, & Future Work	35
4.1	Conclusions	35
4.2	Future Work	36
	Bibliography	37
	Appendix A: WR-5.1 E-H Tuner Drawings	39
	Appendix B: WR-5.1 Waveguide-to-Waveguide MEMS Double Slug Tuner Block Drawings	50
	Appendix C: Python Code for Calculating Slug Sweep Simulation Set- tings	56

List of Tables

2.1	Waveguide parameters.	6
3.1	Fitted Parameters of 20 Sections of MEMS Loaded Silicon Membrane Rectacoax.	24
3.2	Unloaded Transmission Line Simulated Parameters.	24
3.3	Proposed Requirements for WR-5.1 On-Wafer Load Pull Device at DUT.	34

List of Figures

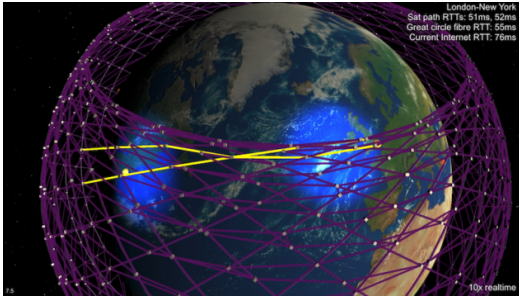
1.2	On-wafer load pull	2
1.3	E-plane and E-plane waveguide tee [8]	4
2.1	E-H Tuner Block Layout and Simulation with Sliding Shorts	7
2.2	WR-5.1 Sliding Short Measurements.	9
2.3	Sliding short dimensions.	10
2.4	Assembled E-H Tuner	11
2.5	Measurement setup for WR-5.1 E-H Tuner.	12
2.6	E-H tuner response at 200GHz, VSWR=13 Circle Drawn, 25 μ m steps	13
2.7	E-H tuner response at 211GHz, VSWR=11 Circle Drawn, 25 μ m steps	14
2.8	A typical circle traced out by sweeping the E- arm while keeping the H- arm fixed. Measured E-H Tuner Response from at 200 GHz with H-sliding shorts set to 0 μ m and E- sliding short swept from 0 to 750 μ m in 25 μ m steps	15
2.9	Simulated Tuning Network Cascade with probe	16
2.10	Measured S-parameters of WR-5.1 Probe used for E-H tuner probe cascade simulation	17
3.1	Schematic Representation of the Load Pull On-Wafer Probe System .	19
3.2	Geometry used for HFSS simulations for parameter fitting	23
3.3	20 section MEMS Loaded Rectacoax Simulation and extraction of unit cell circuit model	24
3.4	WR-5.1 Double Slug Circuit Model Calculations	26
3.5	WR-5.1 Double Slug Circuit Model simulation using simulated fitted parameters and slug length of 3	27
3.6	WR-5.1 Double Slug Circuit Model simulation using simulated fitted parameters and slug length of 2	28
3.7	WR-5.1 Double Slug Circuit Model simulation using simulated fitted parameters and slug length of 1	29
3.8	Proposed Test Structure for WR-5.1 Waveguide Interfaced 23-Section Double Slug MEMS Tuner	30
3.9	Critical Dimensions of WR-5.1 Double Slug Tuner	31
3.10	WR-5.1 Double Slug MEMS Masks sequence	32
3.11	Proposed Layout of WR-5.1 On-Wafer Double Slug Load Pull Device	33

Chapter 1

Introduction

There is interest in performing load pull measurements on millimeter-wave power amplifiers above 100 GHz. These higher millimeter wave frequencies are useful for short range high bandwidth applications. Power amplifiers will need to be designed effectively for high resolution radars operating in the hundreds of GHz range as well as high data rate communication links. For example, SiGe HBT technologies have been used to implement radar imaging system at 210GHz operating with 4-stage power amplifier achieving an output power of +5dBm from an on-chip antenna. The cross-range resolution of this radar was estimated to be 1mm at 775mm distance [1]. An example of a high data rate application would be inter-satellite communication in next generation internet satellite constellations such as Starlink. The effects of atmospheric loss would not be a problem in the vacuum of space.

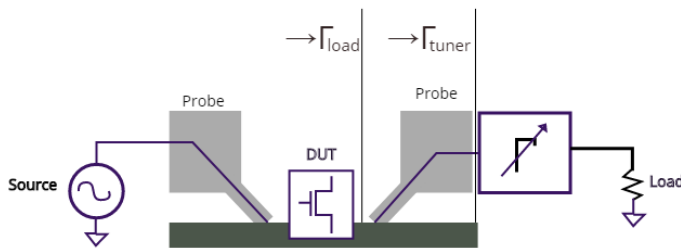
Wireless data links with 10+Gbit/s data rates using quasi-optic uni-travelling carrier techniques at 200GHz at distance of 20cm using 1.5- μ W radiated power [2]. Commercial communication systems offering 10Gb/s wireless data links are already available at E-band (70-80 GHz) [3]. These types of technologies will play important roles in systems such as machine vision for industrial robotics, 5G wireless, inter-satellite communication, and the internet of things.



(a) Starlink mesh satellite network.



(b) An E-band (70/80GHz) millimeter wave system that claims 9.7Gbps capacity.



(a) Load pull Setup



(b) WR-5.1 On-wafer probe

Figure 1.2: On-wafer load pull

1.1 Load Pull Background

Active devices show nonlinear behavior in large signal regime. The power amplifier designer needs to know the input and output power at $f_o, 2f_o, 3f_o$ or more harmonics as a function of bias point and Γ_{load} . Mechanical tuners offer a robust solution for tunable loads due to their simplicity compared to active loads. However any losses in the tuning network cannot be compensated. 0.2dB of interconnect loss reduces Γ

to a maximum of 0.95. Currently, at 110GHz, $\Gamma=0.6$ is possible on wafer after probe losses. Accuracy and repeatability of the probe *Gamma* calibration is necessary if not performing in-situ load measurement [4].

It is necessary to know the real incident and reflected power for a nonlinear measurement. On-wafer measurement allows for removal of device parasitics from measurement. A power calibration is necessary to know the exact powers. The measured powers are limited by the dynamic range of the VNA receivers. More information about the large signal stimulus is gained by measuring harmonics of the fundamental. Error term models with 8-terms can be used to calibrate large signal measurements, however the e01 term cannot be set to unity. Instead it must be calculated using a power sensor as part of the calibration routine or during the measurement [0].

Load pulls have been performed at 300GHz on MMIC amplifiers using varactor or FET tuning elements integrated on wafer. Input matching was also employed to increase the available power at the DUT input. Concern was mentioned about linearity of the matching networks above -3dBm [6].

Electro-optic sampling methods have been proposed and investigated for large signal network measurements at millimeter waves to terahertz frequencies. This method involves sampling a standing wave on a section of transmission line using laser interrogation. [7]

Commercial passive tuners are available that achieve VSWR's of 24:1 up to 110 GHz (WR-10) before probe losses. Constructing a load pull system above 110 GHz poses a significant challenge due to the increased loss and lower available powers from amplifiers for active load synthesis. The impedances generated by a passive impedance tuner are limited by intrinsic tuner losses and interconnect losses between the tuning network and DUT. Thus for a WR-5.1 load pull system it is necessary to construct a tuning network that can achieve high VSWR's in the most compact footprint so it can be integrated as close as possible to an on-wafer probe tip.

1.2 Selection of Tunable Elements for Millimeter Wave Load Pull device

Waveguides are used to connect microwave components at frequencies above 100GHz due to their low loss. Tunable networks are thus reasonably implemented using waveguide based structures. A well studied waveguide junction known as the E-H junction serves this purpose. The E-H junction is a 4-port network which interacts an E-plane arm and H-plane arm together at a single point on a section of waveguide [8]. By tuning the distance of a short circuit from E-plane and H-plane of the junction, it is possible to create an arbitrary impedance transformation. The machining of waveguide blocks at these frequencies is well characterized thus it is reasonable to construct this device through multiple split waveguide blocks. This approach to the on-wafer load pull is taken first.

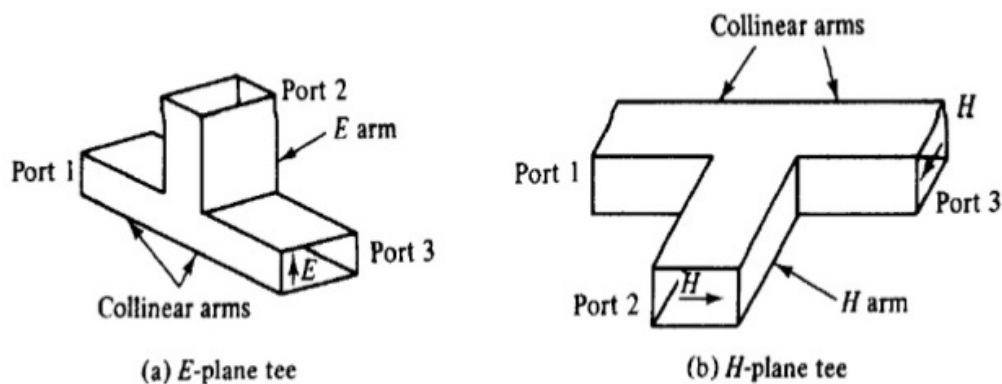


Figure 1.3: E-plane and E-plane waveguide tee [8]

An alternative load pull tuning structure, the double slug topology, is implemented using distributed MEMS loaded transmission line, is proposed next. The distributed MEMS loaded transmission line has previously been demonstrated on quartz substrates at 50GHz [9]. This technique lends itself to being integrated directly on the

silicon membrane probe. The double slug tuner creates impedance transformations through the use of two low impedance sections of transmission line separated by lengths of normal impedance transmission line. By selecting the characteristics of an array of MEMS devices loading a section of transmission line, it is possible to design for the suitable coverage of impedances within a certain VSWR.

Chapter 2

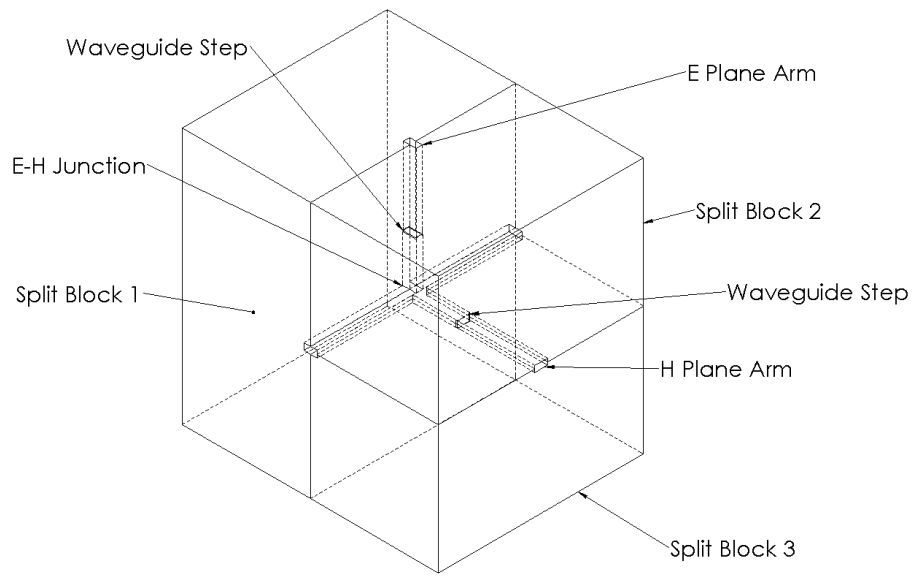
WR-5.1 Waveguide E-H Tuner

2.1 Waveguide E-H Junction Construction

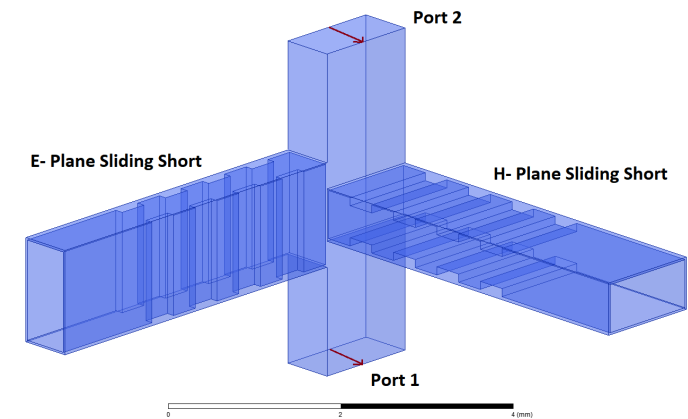
For the WR-5.1 waveguide band (140-220 GHz), a waveguide based E-H junction tuner has been constructed and measured. The block schematics for this device are shown in Appendix A. The standard tolerance available from the machine shop is $\pm 0.0002''$, and this sets the limit on how precisely the microwave properties of the E-H junction can be controlled. The tunable nature of the sliding shorts can compensate for any errors of the junction from nominal geometry, thus the limiting factor of the performance of the device will be the loss of the waveguide sections and sliding shorts. The waveguide portion of the device is constructed of 3 separately milled aluminum blocks. This is necessary due to its 2 protruding waveguide arms from the central through-section of waveguide that connects it to the waveguide flanges. Usually, only 2 blocks are necessary for constructing a waveguide device. The waveguide flanges are designed for the standard WR-5.1 interface as implemented on VDI VNA extenders.

Table 2.1: Waveguide parameters.

Band Designation	Dimension	Frequency Range	Typical WG Loss Low - High
WR-5.1	1.295mm x 0.648mm	140-220GHz	.0185 - .0117 dB/mm



(a) Mechanical layout of E-H Tuner



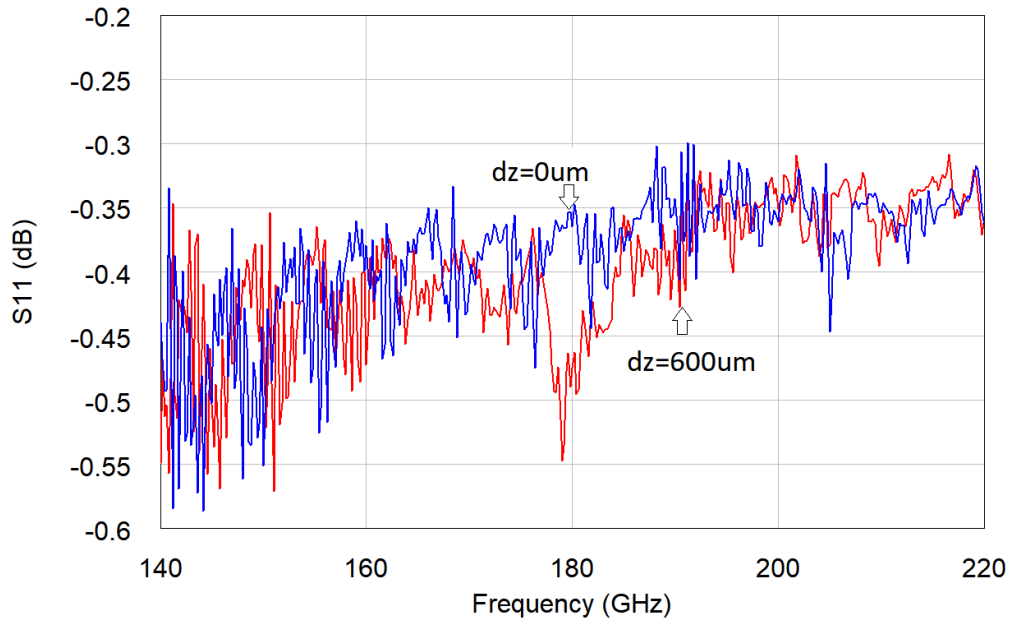
(b) Simulation geometry of E-H Tuner

Figure 2.1: E-H Tuner Block Layout and Simulation with Sliding Shorts

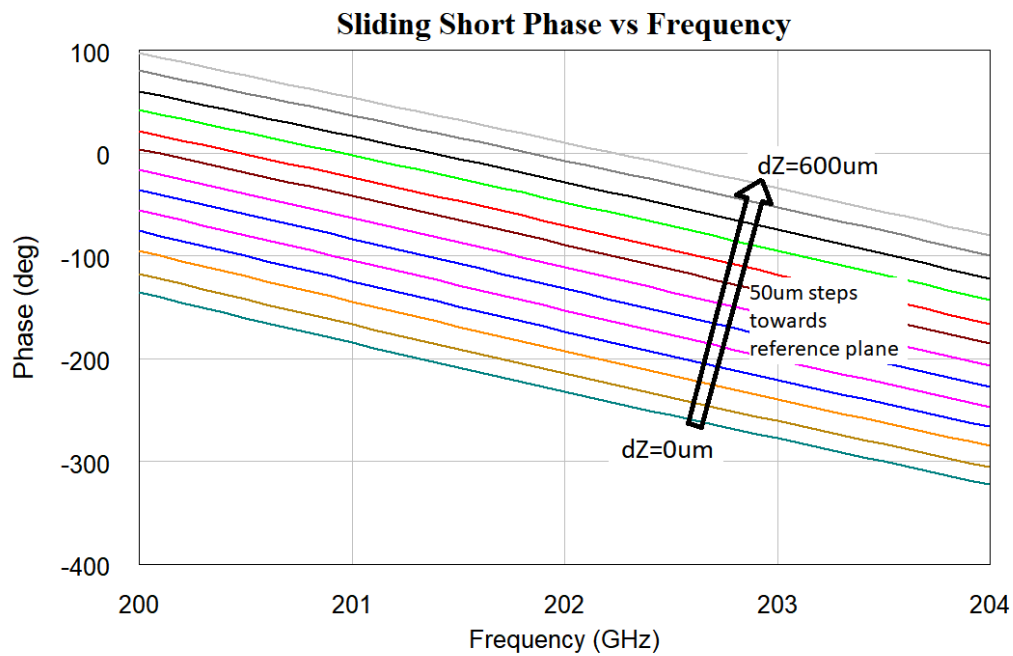
2.2 Waveguide Non-contact Sliding Short

Non-contact waveguide sliding shorts were chosen for the tuner due to their high reliability and performance as seen in prior works [10]. Other works have considered the use of dielectric based shorts [11]. A non-contact sliding short was designed for the WR-5.1 waveguide with four 90-degree high and low impedance sections. The high and low impedance sections are formed by a rectangular-coaxial structure created between the waveguide and a suspended micro-CNC machined metal slug. The sliding short is suspended in the center of the waveguide by machining a step in the waveguide arms. A combination of wire-EDM and CNC milling techniques were used to machine the sliding shorts out of copper. The sliding shorts were inserted into a short section of WR-5.1 waveguide to measure their response. Their position was manipulated with the precision probe station stage. A PNA-X VNA and VDI WR-5.1 VNA extender calibrated with Short-Thru-QW kit was used to make the measurements.

The measured sliding short results exhibit good phase linearity with respect to position. Displacement of the sliding short creates a phase shift of 19.4° per $50\mu\text{m}$ step at 200GHz. The sliding shorts exhibit a typical return loss of 0.35dB. While the return loss could be improved for subsequent designs, these results show this design of sliding short should be acceptable for use in the E-H tuner. The return loss of the tuner could be improved by using high resistivity microfabricated dielectric slugs.

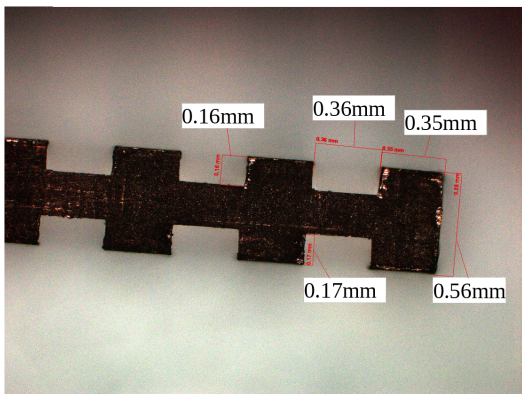


(a) S_{11} of the sliding short at $0\mu\text{m}$ and $600\mu\text{m}$ displacement

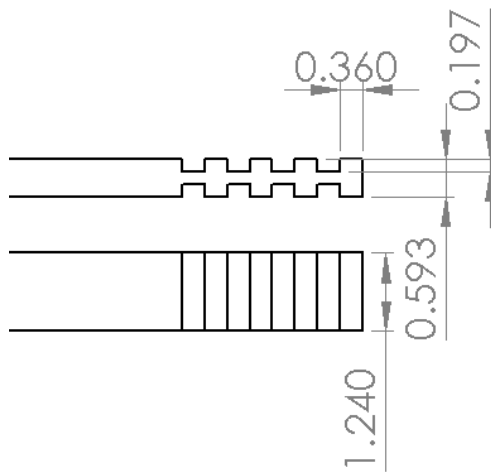


(b) Sliding short Phase vs Frequency through sweep of displacement in $50\mu\text{m}$ steps

Figure 2.2: WR-5.1 Sliding Short Measurements.



(a) Measured Dimensions



(b) Nominal Design Geometry

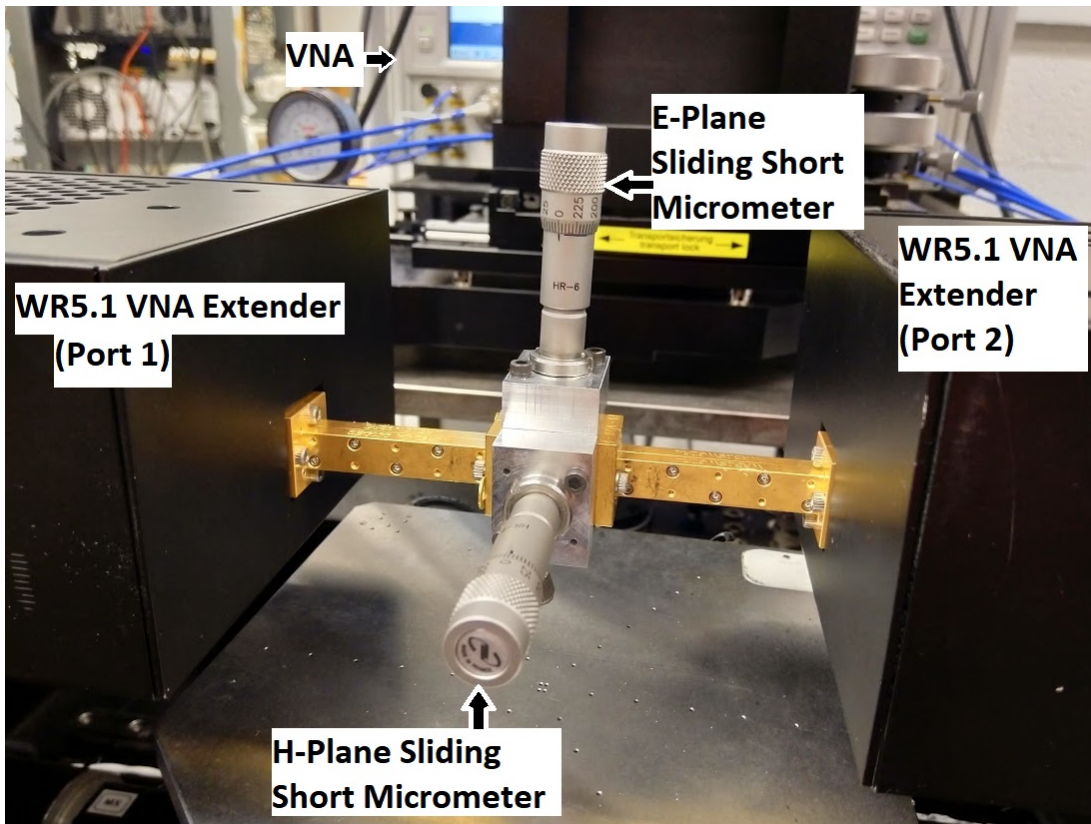
Figure 2.3: Sliding short dimensions.

2.3 E-H Tuner Measurements

The E-H tuner blocks were assembled with the sliding short inserted. The sliding shorts are preloaded against miniature springs for zero backlash. A micrometer is used to push the sliding short towards the junction. The VNA was calibrated and the E-H tuner was connected. The zero displacement reference plane of the E- and H-sliding shorts was found by adjusting the tuners until a good through-response was measured. Then the micrometers were sequentially backed away from the junction in $25\mu\text{m}$ steps. VSWRs above 10:1 were measured at the waveguide reference plane on this device.



Figure 2.4: Assembled E-H Tuner



(a)

Figure 2.5: Measurement setup for WR-5.1 E-H Tuner.

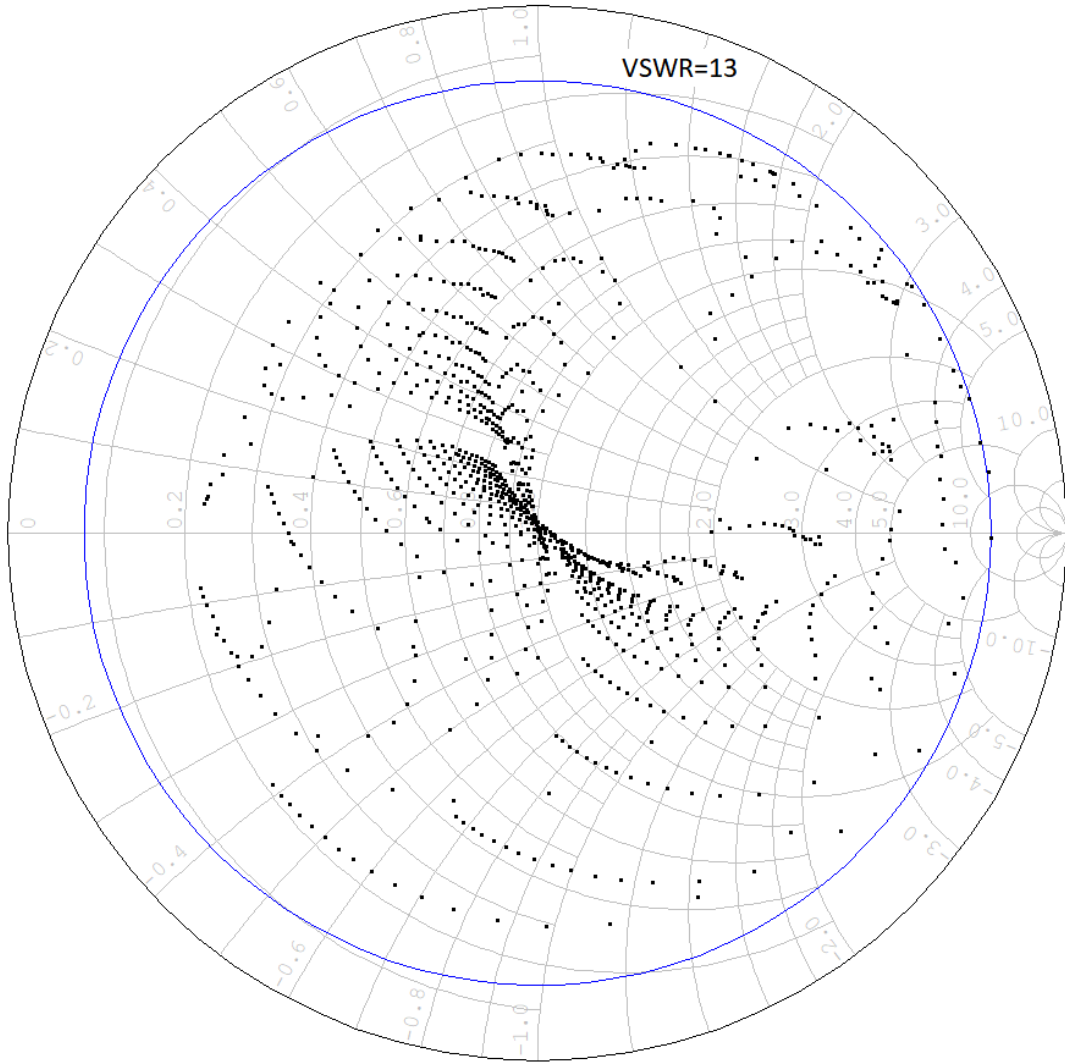


Figure 2.6: E-H tuner response at 200GHz, VSWR=13 Circle Drawn, 25 μ m steps

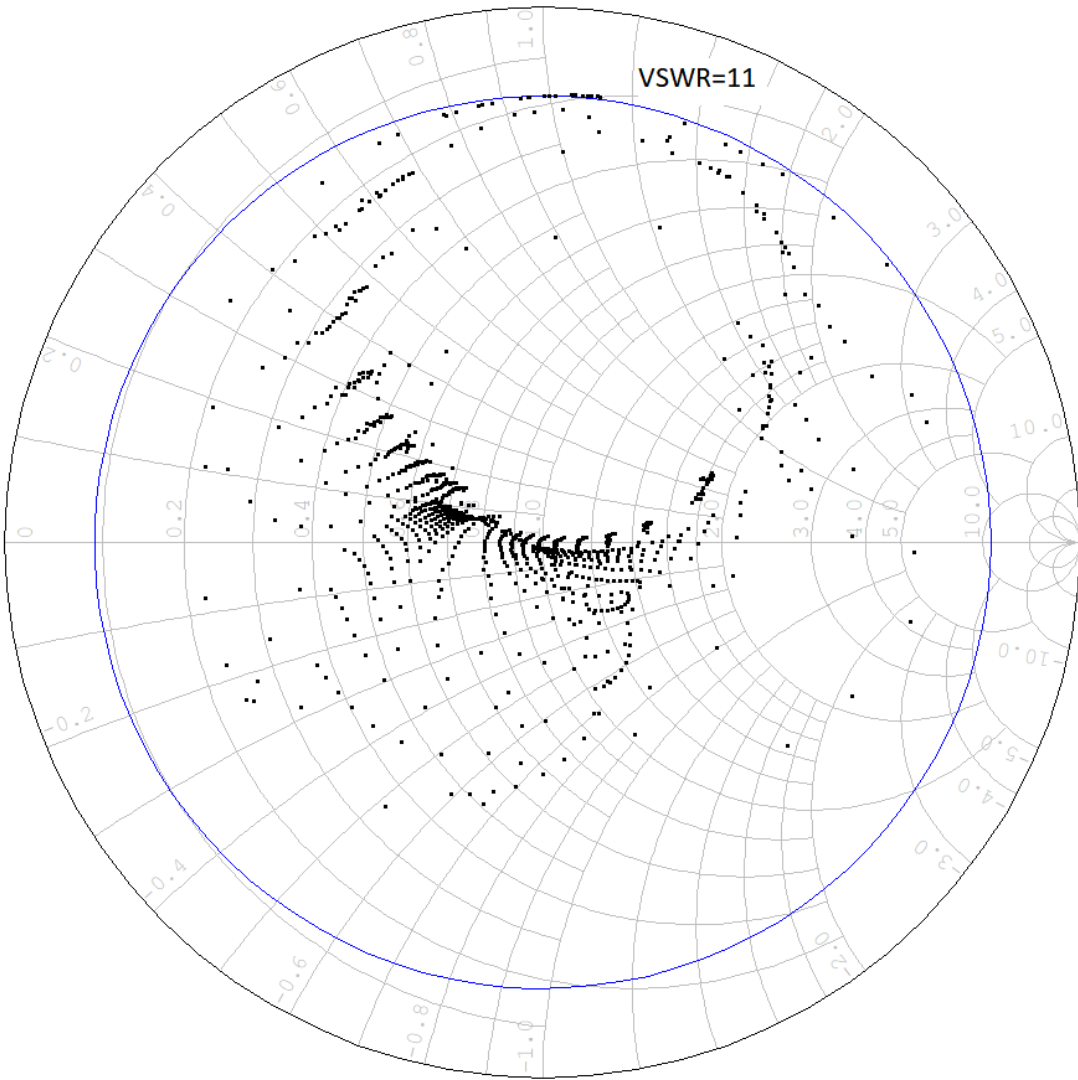


Figure 2.7: E-H tuner response at 211GHz, VSWR=11 Circle Drawn, 25 μ m steps

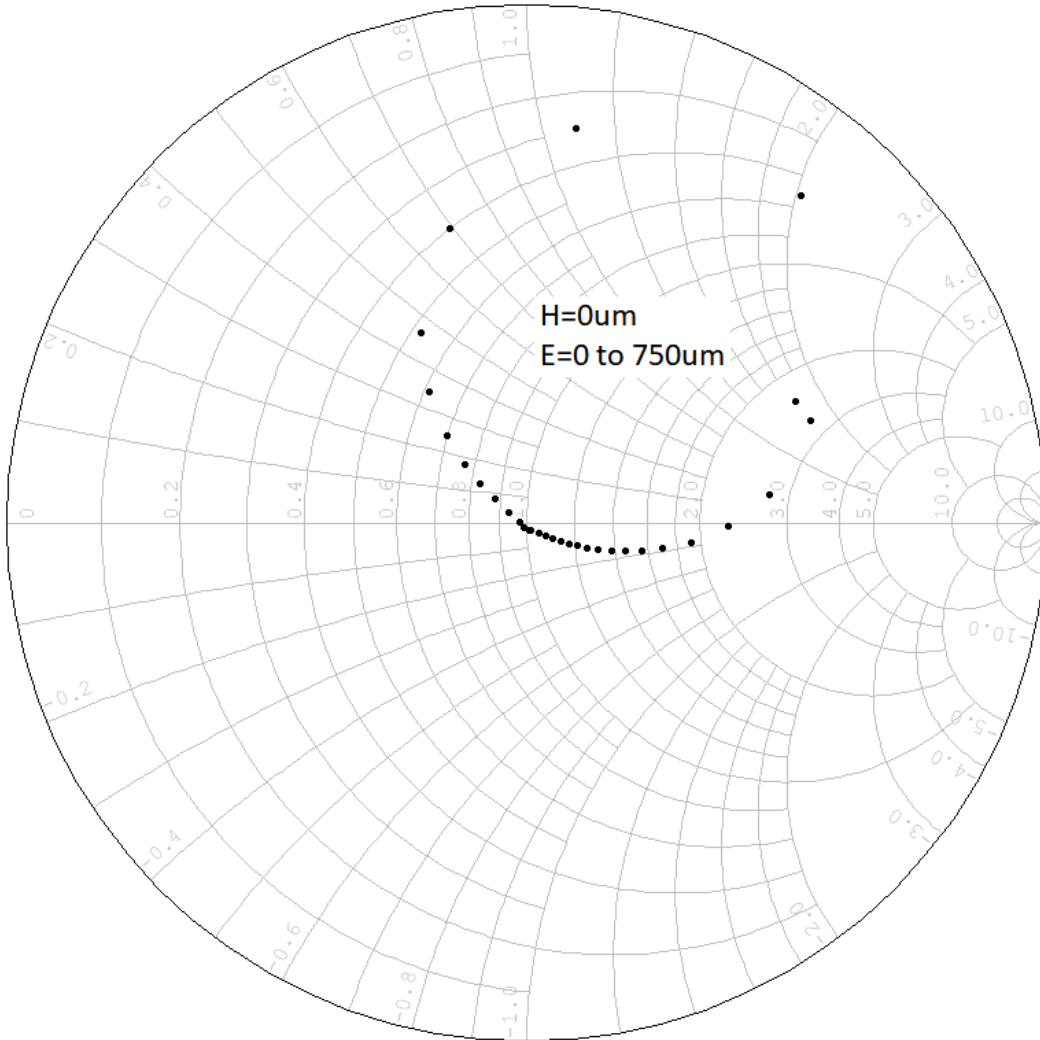


Figure 2.8: A typical circle traced out by sweeping the E- arm while keeping the H- arm fixed. Measured E-H Tuner Response from at 200 GHz with H- sliding shorts set to $0\mu\text{m}$ and E- sliding short swept from 0 to $750\mu\text{m}$ in $25\mu\text{m}$ steps

2.4 E-H Tuner Simulated Network Cascade with Probe

It is shown that this topology could be suitable for tuning waveguide based devices, but its performance in an on-wafer load pull application is limited by the practical integration of the waveguide based E-H junction device close to the on-wafer probe transition and its associated loss. A simulation was performed which cascaded the measured E-H tuner response at the waveguide reference plane with measured WR-5.1 on-wafer probe data. The resulting achievable VSWR's was then noted to be 5.

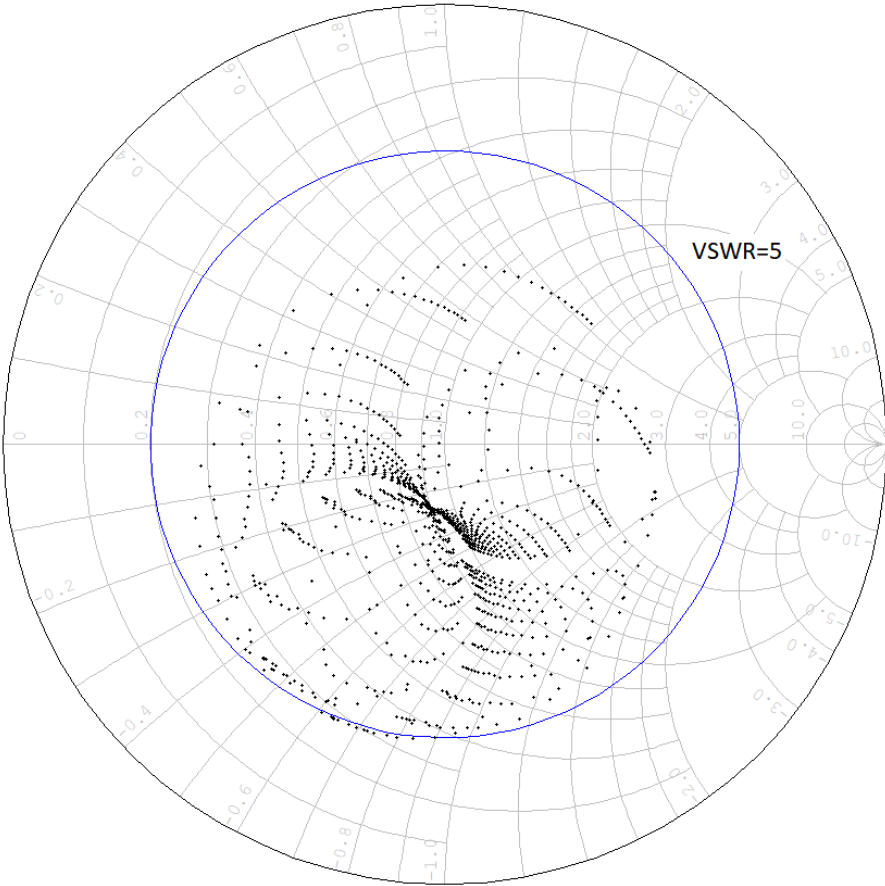


Figure 2.9: Simulated Tuning Network Cascade with probe

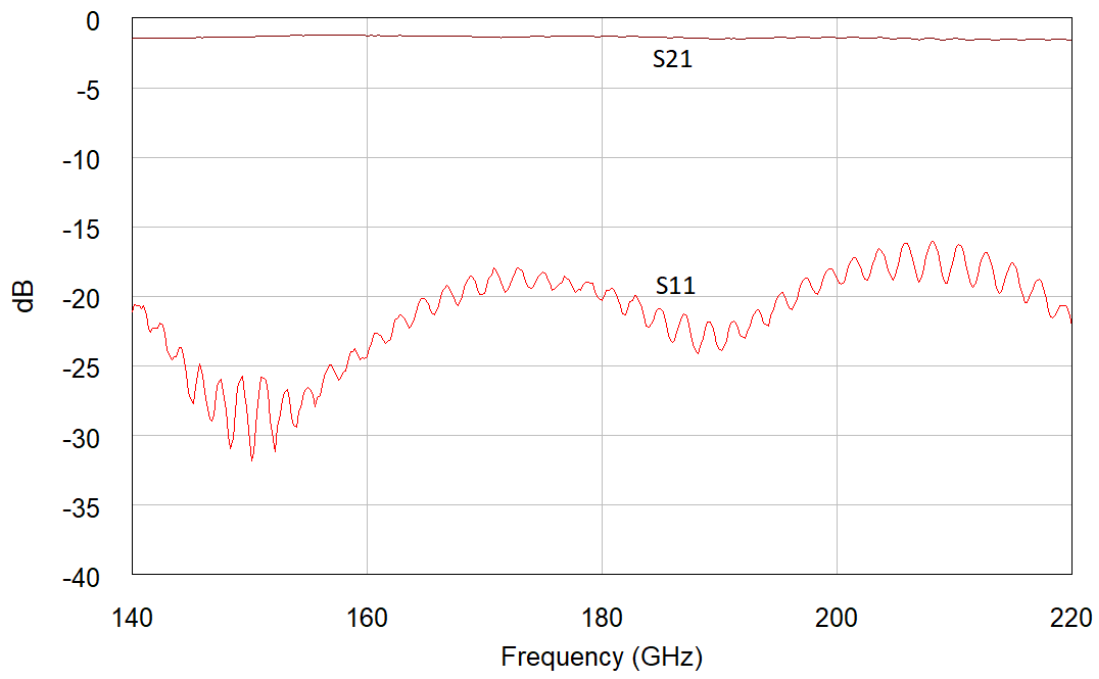


Figure 2.10: Measured S-parameters of WR-5.1 Probe used for E-H tuner probe cascade simulation

Chapter 3

Double Slug MEMS Tuner for On-wafer Load Pull Probe

When a load pull measurement is performed, the tuned load presented to the device is effected by the entire microwave chain connected to the output of the amplifier. The ultimate impedance presented to the device is the result of the system impedance being transformed through the tuning network. Thus reflections between the tuning device and system load must be minimized. Any additional disturbance from the transition between the tuning device and the DUT will also need to be controlled to insure the proper impedances are generated. The effect of the calibration techniques used to determine the system impedance on the load pull output power contours have been investigated in [0]. The schematic of a proposed on-wafer load pull measurement setup is presented in Figure 3.1.

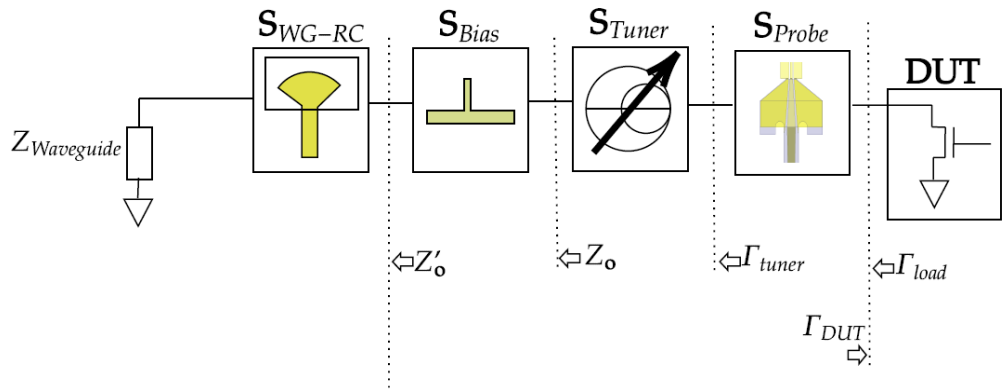


Figure 3.1: Schematic Representation of the Load Pull On-Wafer Probe System

3.1 Double Slug MEMS Device Simulations

In order to improve the performance of the tuning at the on-wafer reference plane, an alternative topology was needed. MEMS minimal contact fixed-fixed airbridge capacitors provide the suitable quality factors and capacitances needed for implementing a tuning network on silicon membrane process for integration in a probe. They are also robust against large signal nonlinear effects that will occur during load pull measurements due to their high actuation voltages.

The actuation voltage of a MEMS device is determined by the energy associated with its capacitance and voltage and energy stored in the bending and stretching of the thin air-bridge beams. The mechanical energy is described with the spring constant k associated with the vertical displacement of the air bridge, and is effected by the elastic modulus E , thickness t , width w , length l , initial height h_o , actuated height h , and residual stress σ of the beam [9].

$$k = 2Ew(t/l)^3 + Ewt(h_o - h)^2/l^3 + 2\sigma(1 - \nu)tw/l \quad (3.1)$$

The energy from the applied voltage and capacitance of the air bridge is best found by performing 3D electrostatic simulations due to the strong fringing effects occurring at small bridge dimensions necessary for achieving the small capacitances needed for the double slug operation. Because of this, the actuation voltage is only roughly calculated given the vacuum permittivity ϵ_o and center conductor width W as

$$V = \frac{2k}{\epsilon_o W w h^2 (h_o - h)} \quad (3.2)$$

A full electromagnetic simulation of the device is necessary to extract the capacitance and also the inductance.

3.2 Double Slug Tuner Theory

The microwave properties of the tuner are determined by the unloaded transmission line parameters, the MEMS bridge capacitances and parasitics, the spacing of MEMS

sections, and number of sections. The unloaded transmission line properties can be extracted from HFSS simulation.

The loaded per unit length capacitance and inductance of the transmission line are calculated, with c being the speed of light in vacuum.

$$C'_{loaded} = C_{eff}/s + C'_{unloaded} = C_{MEMS}/s + \frac{\sqrt{\epsilon_r}}{cZ_{unloaded}} \quad (3.3)$$

$$L'_{unloaded} = C'_{unloaded}Z_{unloaded}^2 \quad (3.4)$$

It is important to note the effective capacitance of the MEMS device due to the series inductance of the MEMS bridge. This effect can significantly disrupt the tuner performance if not controlled.

$$C_{eff} = \frac{C_{up/down}}{1 - \omega^2 L_{bridge} C_{up/down}} \quad (3.5)$$

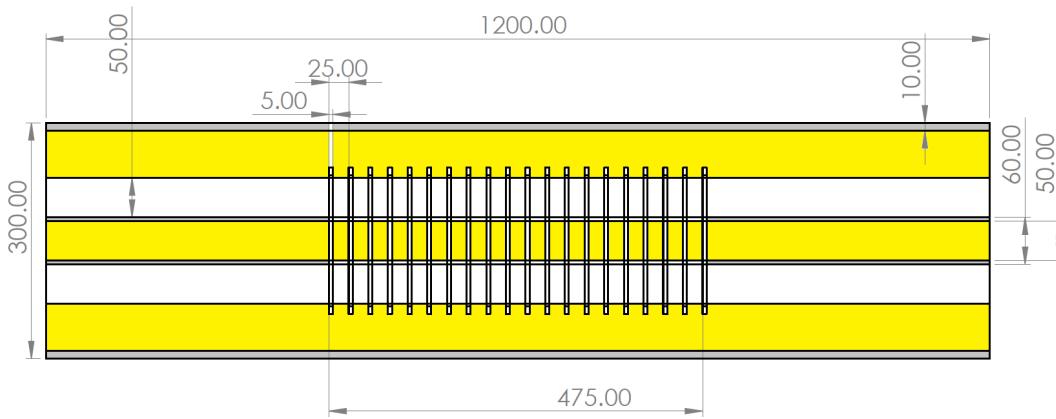
The effective characteristic impedance and propagation velocity of the transmission line is then calculated for the loaded line for the actuated and unactuated capacitances. The maximum VSWR created by the device is then calculated, assuming two quarter wavelength slugs are spaced a quarter wavelength apart.

$$VSWR_{max} = \frac{Z_o^4}{Z_m^4} \quad (3.6)$$

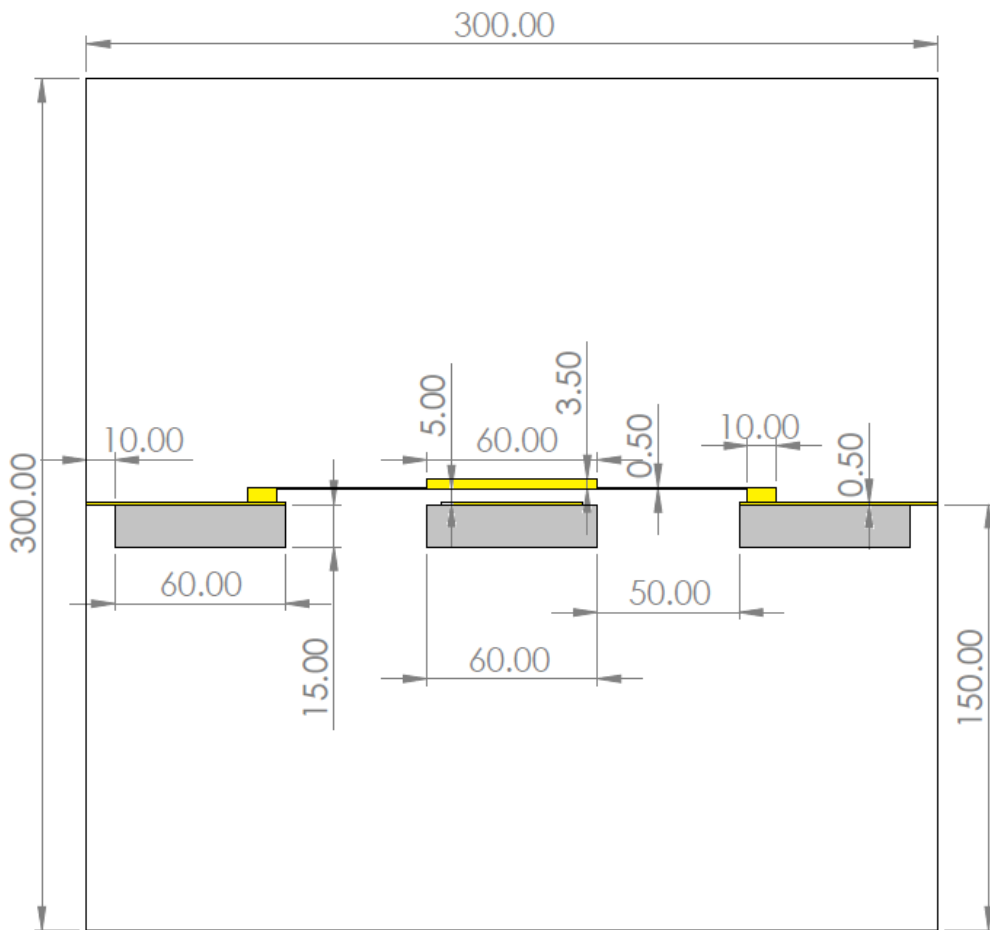
The choice of number of sections, section length, loading capacitance, and unloaded characteristic impedance determine the tuner performance. These selections must also take into account the physical constraints of the fabrication of the MEMS bridges. In general, the higher the number of sections to generate an effective quarter wavelength of length, the greater the resolution of the tuner. The most favorable initial design would pick the smallest number of slugs to cover the selected waveguide bandwidth, yet still provide suitable coverage at the low end frequency of the waveguide since that will require the greatest number of loaded sections to create the quarter wavelength sections.

3.3 Design of WR-5.1 MEMS Double Slug Tuner on Silicon membrane

An example of a design for initially testing this tuning network is as follows. Unit cell fittings of full 3D HFSS simulations of 20 sections of loaded rectacoax were performed. A rectacoax transmission line was simulated using $15\mu\text{m}$ thick silicon as a substrate. A rectacoax cavity dimension was chosen to be $300\mu\text{m}$ by $300\mu\text{m}$. Higher order mode cutoff is assured by proper sizing of the cavity dimension and checked by HFSS simulation. The silicon membrane is suspended in the middle of the channel by the ground beamleads clamped by the split block. A gap in silicon membrane between center conductor and ground was necessary to reduce parasitic capacitance of the MEMS airbridge. The parasitic capacitance is due to the fringe fields in the high dielectric constant silicon and has the effect of reducing the effective capacitance ratio of the MEMS device. Achieving the smallest possible capacitance is also important to increase the self resonant frequency of the device. The width of the MEMS air bridge was selected to be $5\mu\text{m}$. The height of the air bridge was then varied to see the variation of capacitance. Fitted values of capacitance and series inductance were found to be in the range of 1.5-20fF and 20-40pH.



(a) Top View of 20 Sections of loaded line used for fitting unit cell parameters



(b) Side View

(c) Simulation Geometry of Silicon Membrane Rectacoax for Unit Cell Fitting. Dimensions in μm . White=Air, Gold=Gold, Grey=Silicon

Figure 3.2: Geometry used for HFSS simulations for parameter fitting

Table 3.1: Fitted Parameters of 20 Sections of MEMS Loaded Silicon Membrane Rectacoax.

Parameter	Simulated Fit Value	Description
C_{up}	1.75fF	Unactuated capacitance
R_{bridge}	6Ω	Bridge resistance
L_{bridge}	34 pH	Bridge inductance

Table 3.2: Unloaded Transmission Line Simulated Parameters.

Parameter	Simulated Value	Description
ϵ_r	1.276	Transmission line dielectric constant
α	16.4/17/17.8	Transmission line loss at Np/m 140GHz/180GHz/220GHz

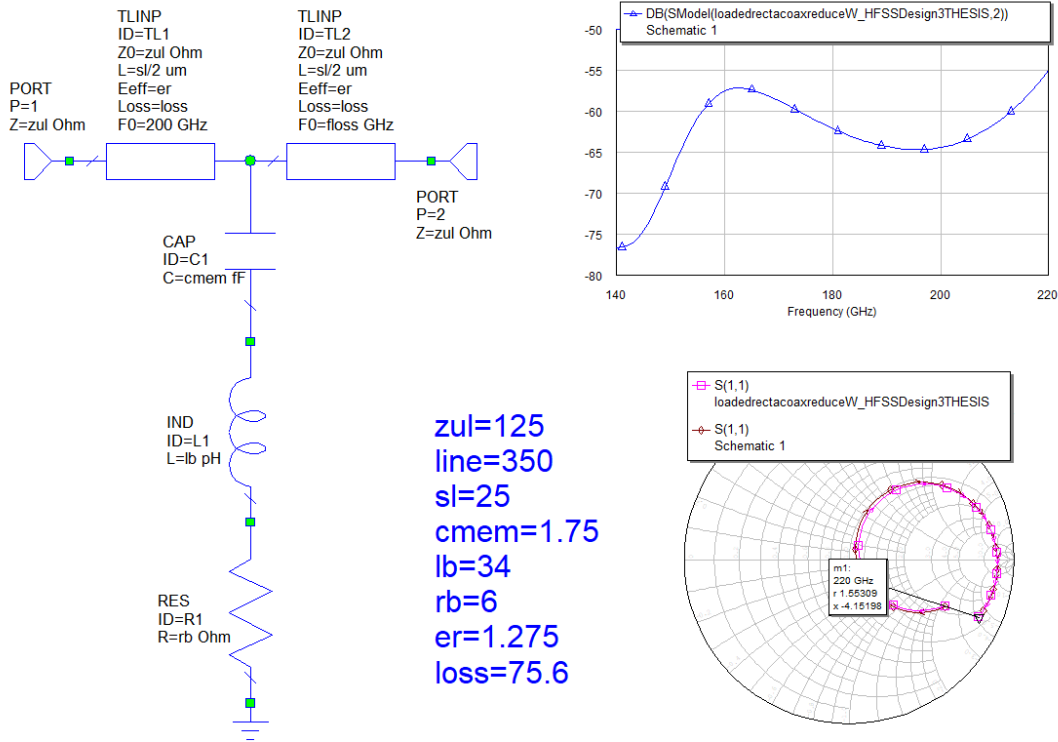


Figure 3.3: 20 section MEMS Loaded Rectacoax Simulation and extraction of unit cell circuit model

Based on the extracted unit cell parameters, calculations were performed to find the section length and capacitance ratio. The desired number of actuated MEMS capacitors to form the low impedance slugs is chosen based on the WR-5.1 waveguide bandwidth and the need to reduce the number of devices to the minimum amount required to demonstrate the device. The minimum slug lengths of 3,2,1 corresponding to maximum VSWR performance at 140, 180, and 220GHz were selected. A table of the necessary calculations was constructed.

Lambda (m)										
0.00214285714										
Omega (rad/s)	freq (Hz)	Cup (F)	Cdown (F)	Cratio	dielectric const.	Zunloaded (Ohms)	C' (F/m)	L' (H/m)	Series Inductance (H)	
879645943005	1.40E+11	1.75E-15	8.75E-15	5	1.275	125	3.011091E-11	4.704829E-07	3.40E-11	
Creff	s (m)	CupL	CdownL (F)	C'effup	C'effdown	Zup	Zdown	VSWR		
6.19614575352	6.00E-05	1.834458E-15	1.1367E-14	6.0685E-11	2.1955372E-10	88.0502336363309	46.29152896	13.08928577		
Prop. Velocity eff. Up (m/s)	Prop. Velocity eff. Down (m/s)	Effective dielectric const. Up	Effective dielectric const. Down	Effective lambda up (m)	Effective lambda down (m)	Effective beta up (rad/m)	Effective beta down (rad/m)	Theta up (deg)	Theta down (deg)	
187148634.201	98391521	2.569621666	9.29666454	0.00133678	0.00070279658	4700.25307297665	8940.261653	16.15827982	30.7343556268	
n90up	n90down	n180up	n180down	Ntotal	total length (micrometers)					
5.5698998274	2.92831908	11.13979965	5.85663816	22.5663376	1353.98025856					

Figure 3.4: WR-5.1 Double Slug Circuit Model Calculations

The premise of these calculations is to determine the phase change of a loaded or unloaded section. The effective propagation constant is found based on the effective capacitance and inductance per unit length of transmission line. Once the phase change per actuated and unactuated section is known then the total number of sections is calculated as $2N_{90down} + 3N_{90up}$ at the lowest frequency of the waveguide band - 140GHz. The circuit model with the total number of sections is then simulated. The code for generating the slug sweep parameter file is shown in Appendix C. This enables all possible double slug configurations for a particular slug length to be evaluated in simulation. The following pages display the proposed tuner performance given the section length of $60\mu m$, capacitance ratio of 5, with the system impedance of 86Ω .

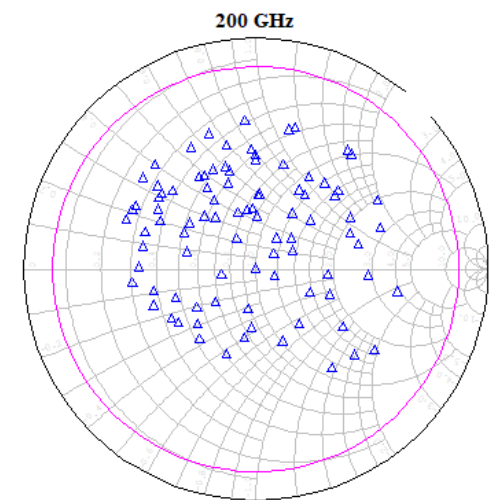
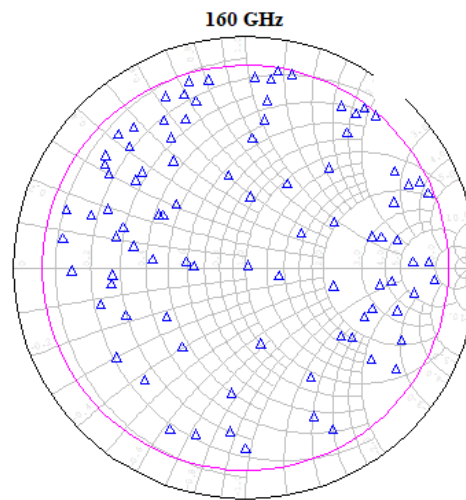
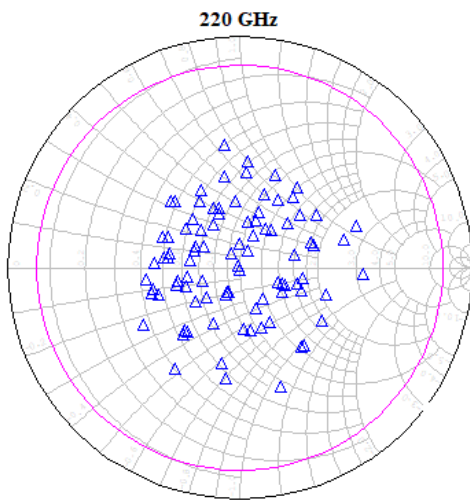
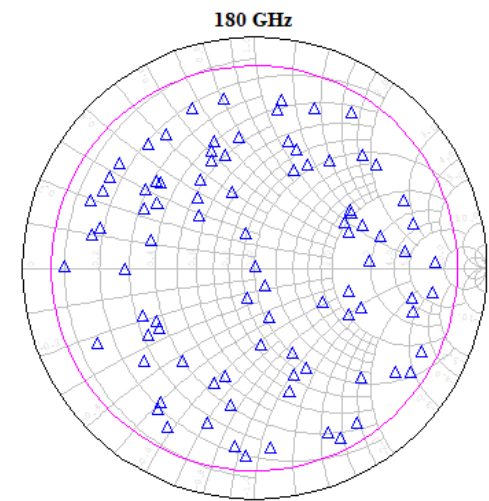
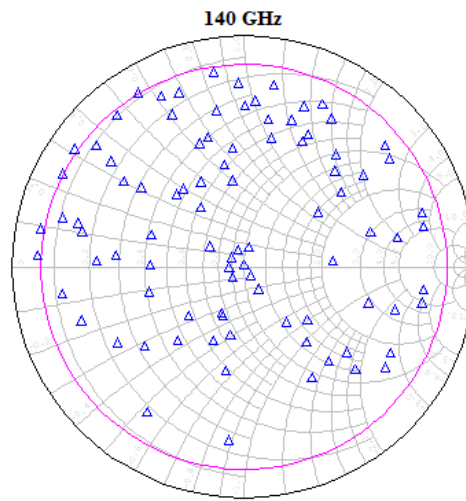
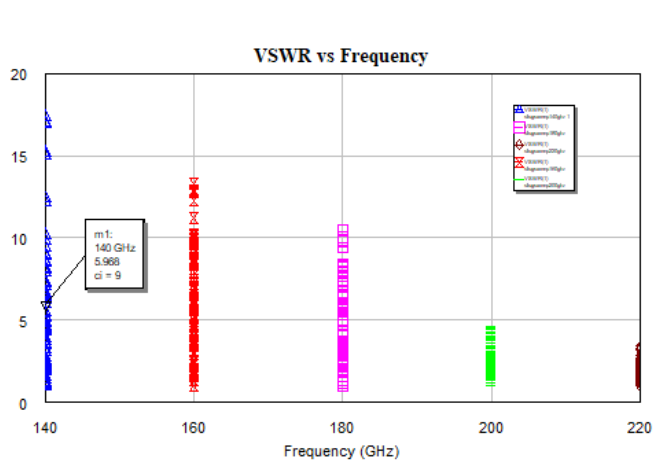


Figure 3.5: WR-5.1 Double Slug Circuit Model simulation using simulated fitted parameters and slug length of 3

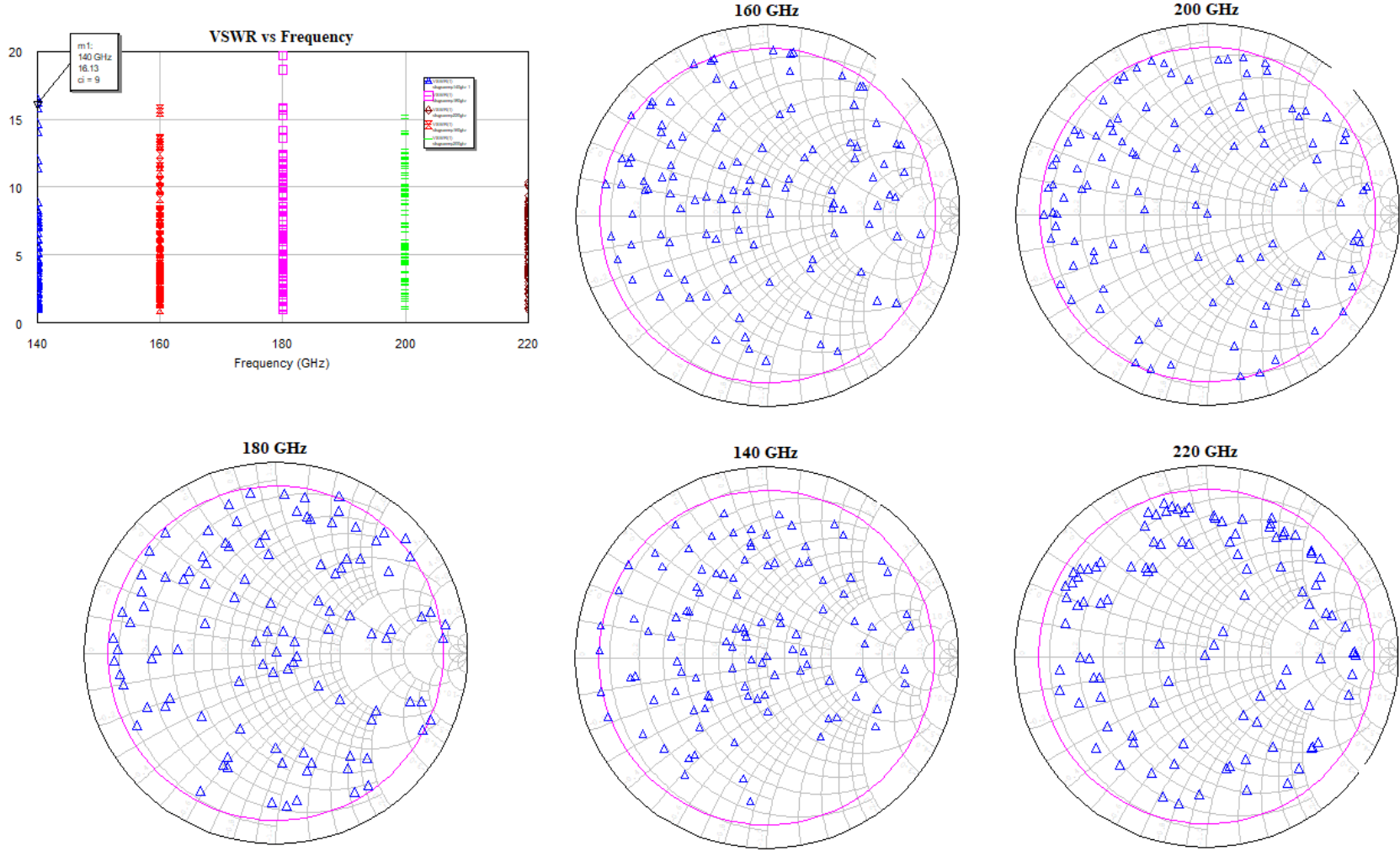


Figure 3.6: WR-5.1 Double Slug Circuit Model simulation using simulated fitted parameters and slug length of 2

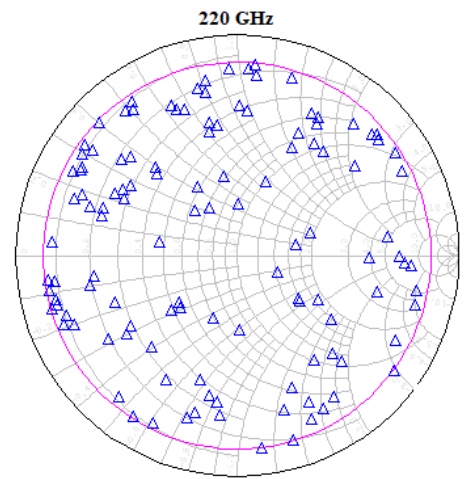
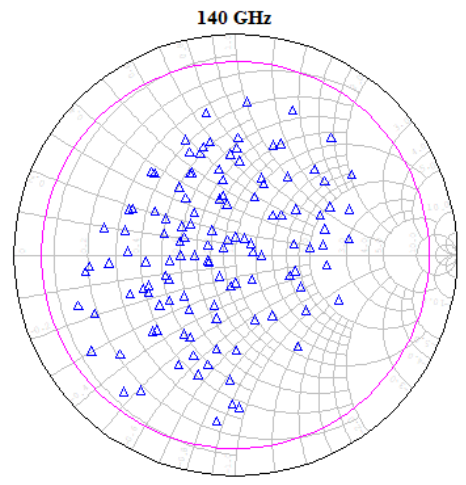
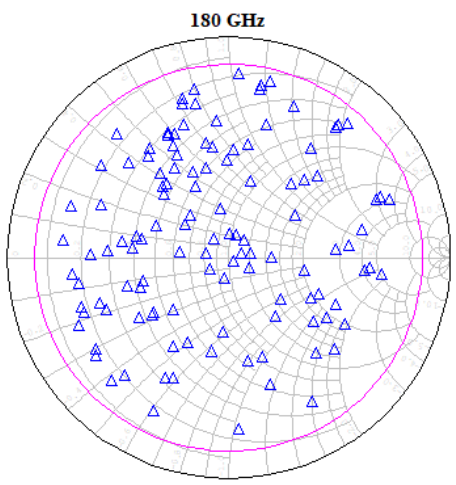
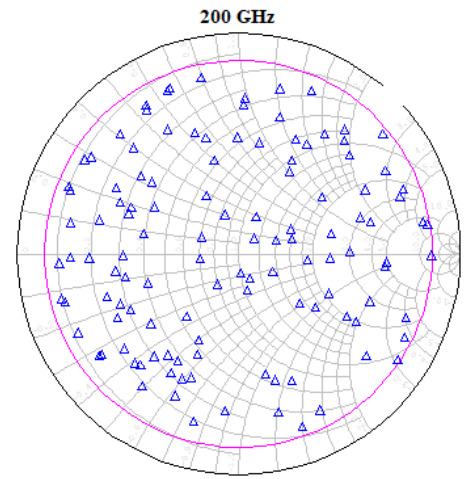
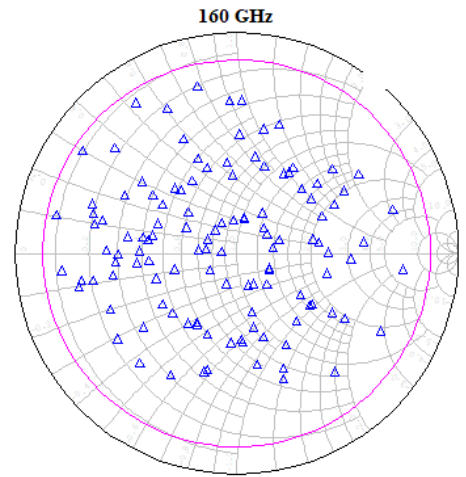
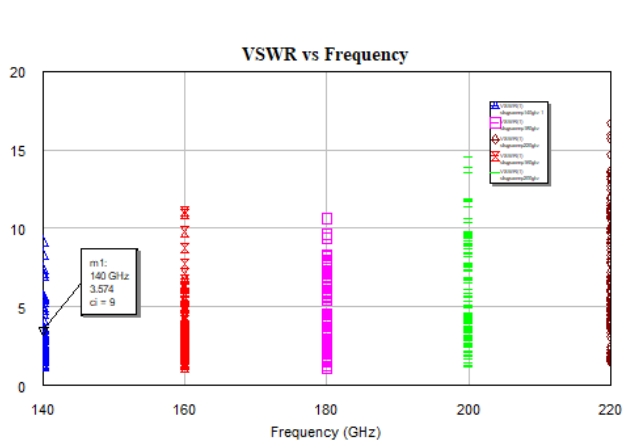


Figure 3.7: WR-5.1 Double Slug Circuit Model simulation using simulated fitted parameters and slug length of 1

3.4 Proposed Geometry and Fabrication of WR-5.1 Double Slug Tuner Test structure and On-Wafer Probe

The practical implementation of a test structure for the double slug MEMS tuner requires input and output radial stub transitions to WR-5.1 waveguides. A calibration will be performed at the waveguide interface and measured impedances of such a device will be relative to the waveguide system impedance. An array of beamleads are required to connect biasing voltages to each MEMS device. High quality ALD- Al_2O_3 MIM capacitors are required for each MEMS device. The thickness of the dielectric will be selected to prevent breakdown under the applied actuation voltage of the MEMS devices. Breakdown fields of 7MV/cm are reported for ALD Al_2O_3 [0]. Bias voltages above 100V may be required based on initial simple calculations of bridge capacitance and bridge spring constants. Note that bias capacitance of 1.25pH was added to the double slug circuit model simulation in the previous section, corresponding to $50\mu m \times 50\mu m$ of capacitor area at 175nm thick with $\epsilon_r = 10$ per section.

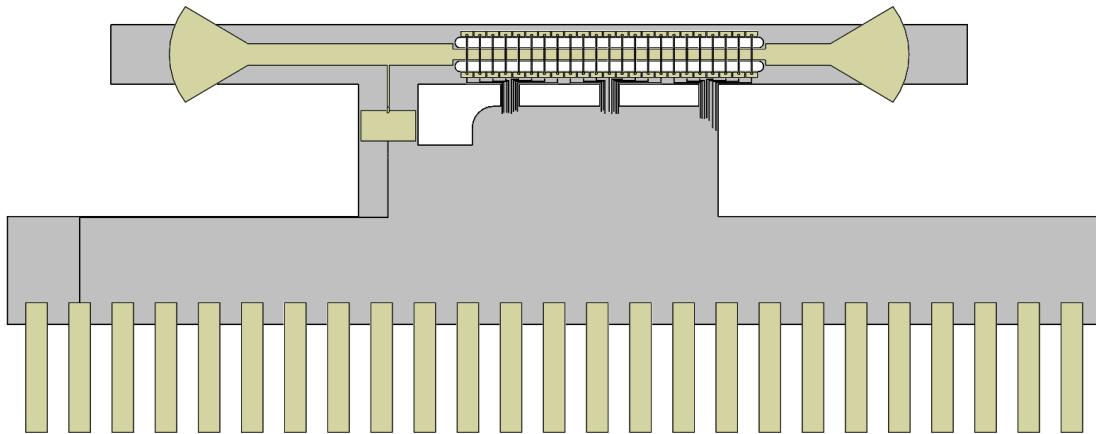
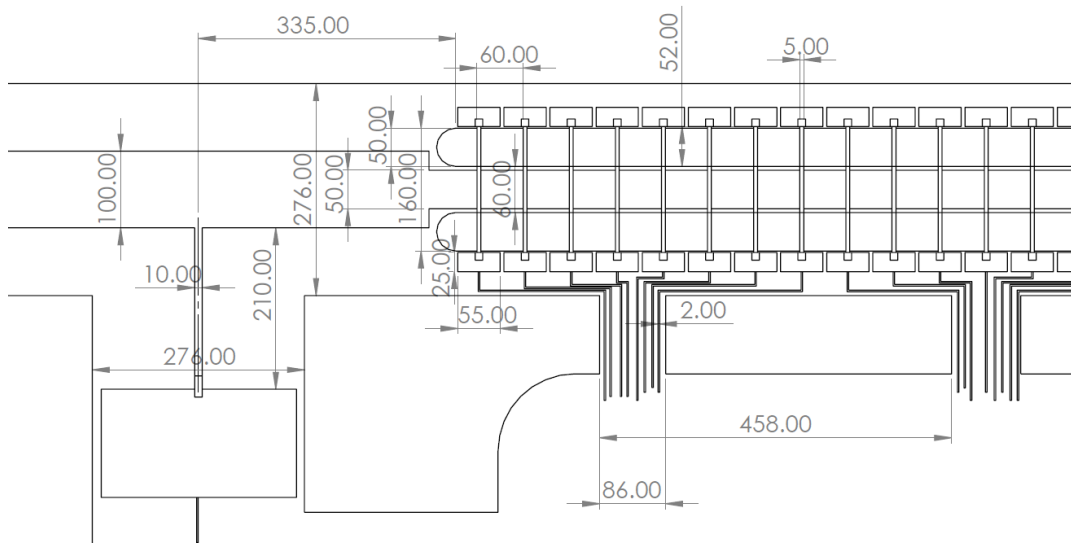
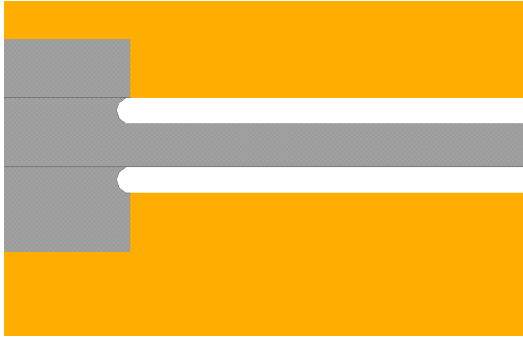


Figure 3.8: Proposed Test Structure for WR-5.1 Waveguide Interfaced 23-Section Double Slug MEMS Tuner

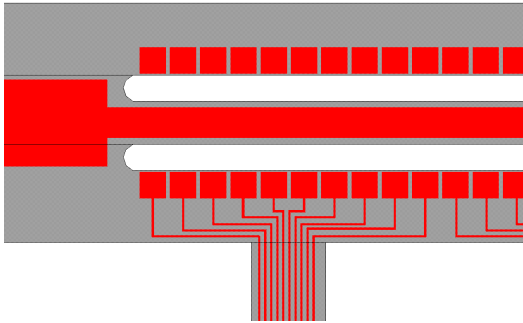


(a)

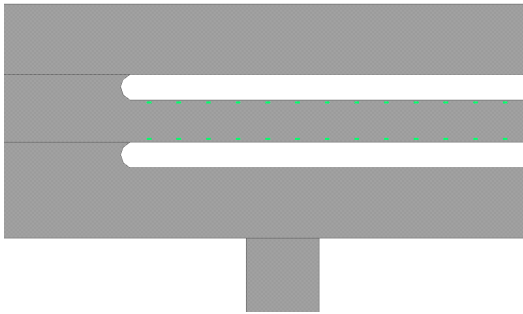
Figure 3.9: Critical Dimensions of WR-5.1 Double Slug Tuner



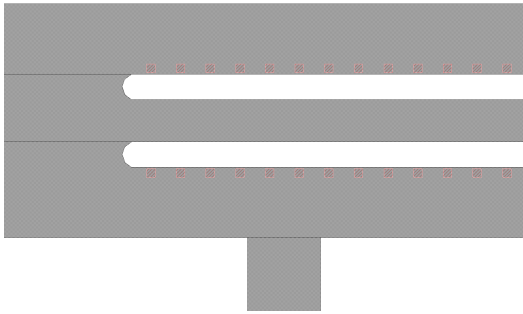
(a) Mask 1 - Liftoff RF Ground Beam-lead



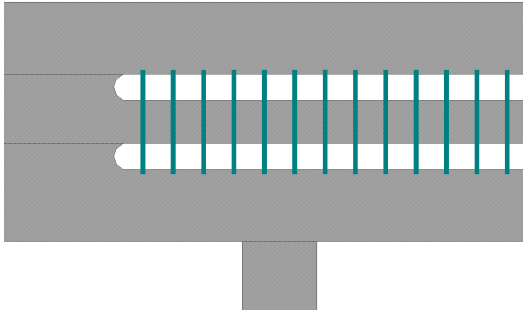
(b) Mask 2 - Perform ALD of Al₂O₃ and Liftoff of MIM top electrode liftoff



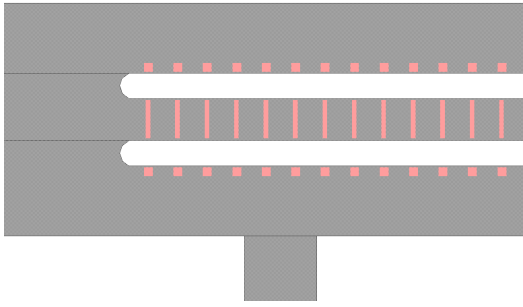
(c) Mask 3 - Etch Aluminum Sacrificial Layer for Bridge Standoff



(d) Mask 4 - Etch Aluminum Sacrificial Layer for Bridge Anchor



(e) Mask 5 - Evaporate Liftoff Gold for MEMS Bridge



(f) Mask 6 - Plate thick section of MEMS bridge and bridge anchors



(g) Mask 7 - Silicon Extent etch

Figure 3.10: WR-5.1 Double Slug MEMS Masks sequence

If such a test structure proved effective at demonstrating the double slug tuning at the WR-5.1 waveguide interface, then the following probe layout could be considered for future work. The limiting factor of the maximum VSWR that can be presented on-wafer is therefore the performance of the rectacoax to on-wafer CPW probe transition. Minimization of the reflection, radiation, and resistive loss in this transition will be critical to the performance of the tuner. Given a VSWR of 20 produced by the MEMS double slug tuner, an $|S_{21}|$ of 0.95 is required for VSWR's of 10 to be presented to the DUT.

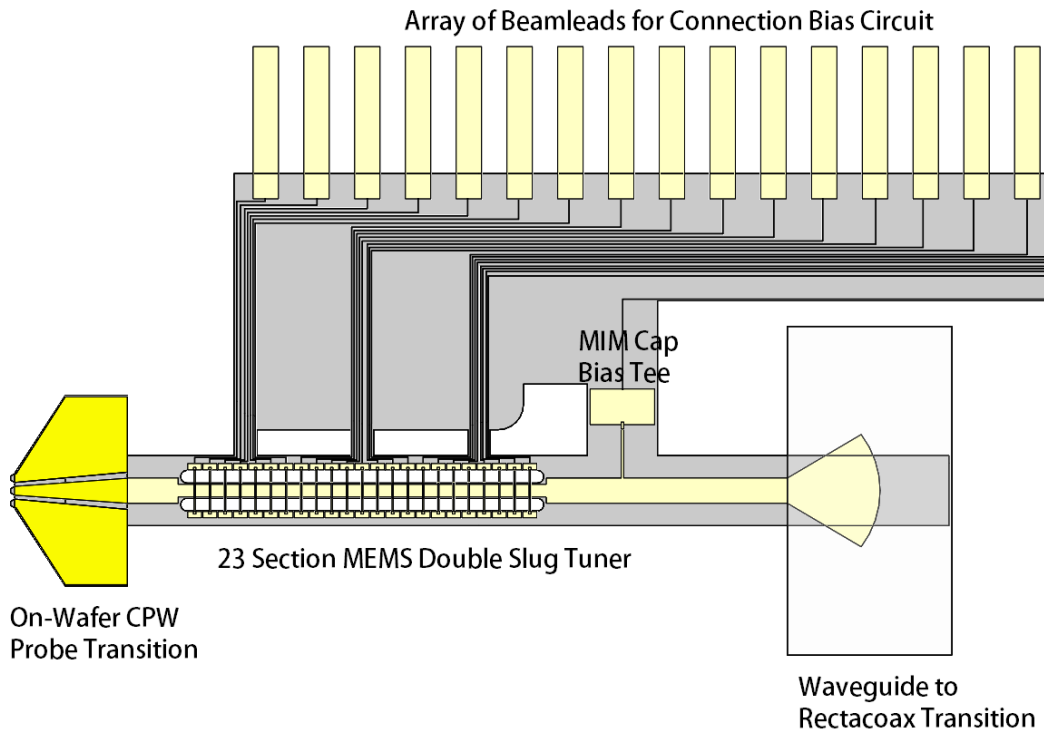


Figure 3.11: Proposed Layout of WR-5.1 On-Wafer Double Slug Load Pull Device

Table 3.3: Proposed Requirements for WR-5.1 On-Wafer Load Pull Device at DUT.

System Impedance	VSWR at Tuner	Probe Transition S_{21}	VSWR at DUT
87Ω	20	0.95	10

Chapter 4

Conclusions, Recommendations, & Future Work

4.1 Conclusions

Load tuning up to VSWR-10 was demonstrated using an E-H junction with non-contact sliding shorts for the WR-5.1 band. Since this device was constructed using conventional CNC machining techniques, it would be feasible to integrate it into an on-wafer probe which is constructed using the same process. It would be necessary to integrate a servo tuning mechanism for each arm to precisely control the location of the sliding shorts. This may prove difficult due to the limited room available close to the probe tip and the size of available actuators and linear encoders. Additional complications are required for the software algorithm due to the sensitive response of the network to the geometry of the E-H junction. A model for the junction would have to be extracted as a function of sliding short position with fine resolution. This resolution is more than what can be accomplished by hand. An interpolation algorithm would be necessary to calculate the location of the sliding shorts for the most exact impedance values. In a load pull application, an accuracy of $\pm 1\Omega$ may be required.

Due the required waveguide interface of the current VNA extender, current on-wafer load pull capabilities are limited to the so called 'non-real-time' load pull configuration. This is due to the inability to put the directional couplers of the VNA between the tuner and the DUT in current WR-5.1 probes [0]. Calibration of the

load pull requires a sequence of VNA-like calibration and a power calibration. In non-real-time systems, the uncertainty of the load pull measurements are caused by VNA calibration uncertainty, connector repeatability, and tuner repeatability [4]. Because of this, the probe contact and tuner repeatability are essential for high quality on-wafer load pull results.

Due to the waveguide tuner limitations, it was necessary to look at alternative techniques such as the double slug MEMS tuner. Since the MEMS device and transmission line geometries can be well controlled and integrated directly on the probe, this topology would provide excellent control over the tuning process. Based on previous work, simulations were performed to model the MEMS air bridge actuated and unactuated capacitances. The parasitic inductance and resistance of the bridges was also extracted from the simulated data. VSWR's of 10:1 should be possible at the DUT reference plane given a tuner VSWR of 20:1 and a minimum rectacoax to on-wafer-CPW probe transition $|S_{21}|$ of 0.95 (assuming no reflections at this interface).

4.2 Future Work

The double slug MEMS tuner proposed should be feasibly integrated into existing on-wafer WR-5.1 probe recipes. Further investigation into the maximum breakdown voltage of the MIM dielectric should be made as this will determine the effectiveness of the MEMS actuator by allowing a short and stiff bridge with low inductance. Additional care will need to be taken to perform the MEMS sacrificial release using critical point drying or dry etching. If these challenges in fabrication can be overcome then a suitable on-wafer load pull system could be implemented which would be extremely useful in enabling high performance power amplifier design for future 5G and millimeter wave systems.

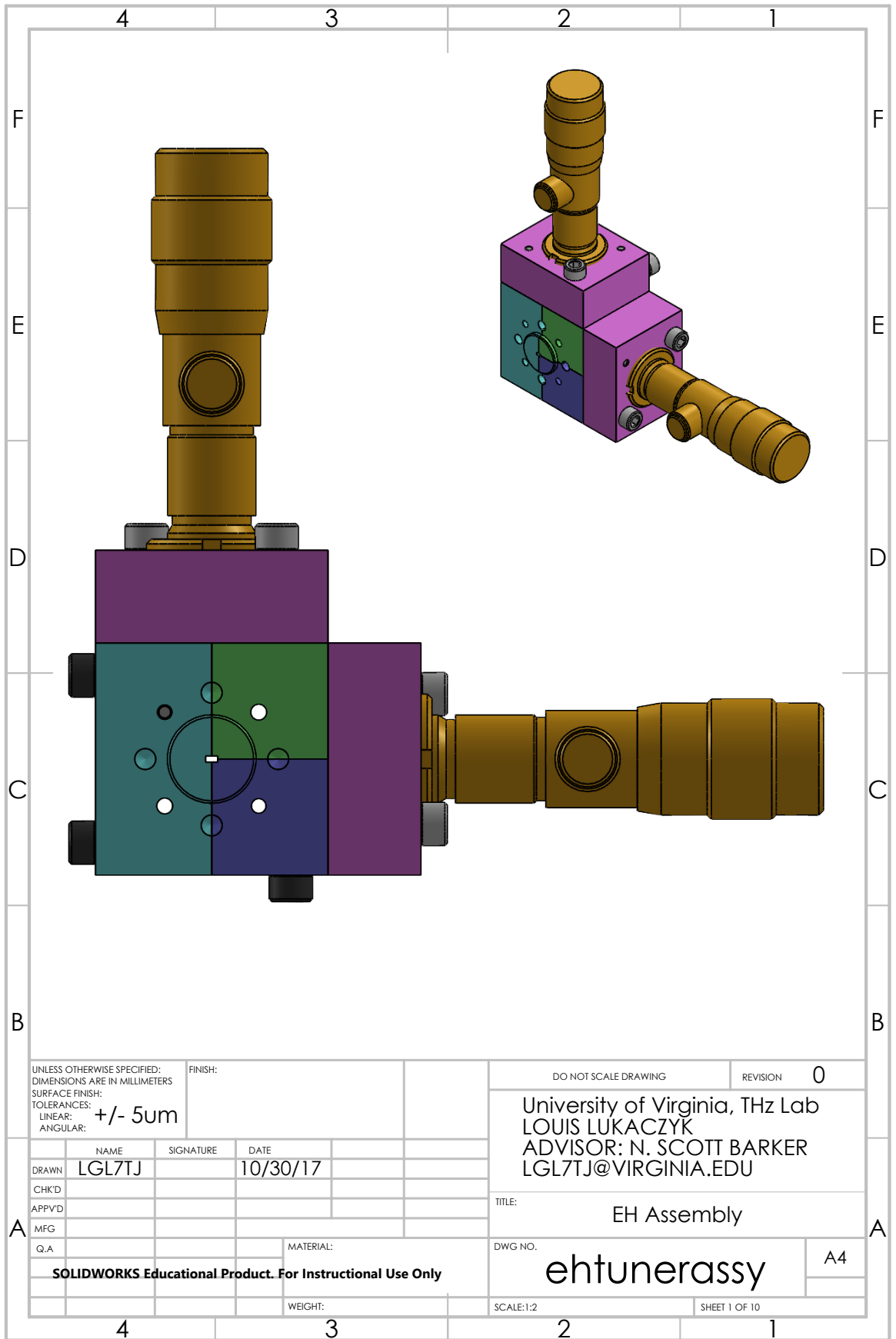
Bibliography

- [1] J Grzyb, K Statnikov, N Sarmah, and U. Pfeiffer, “3-d high-resolution imaging at 240 ghz with a single-chip fmcw monostatic radar in sige hbt technology,” in *2016 41st International Conference on Infrared, Millimeter, and Terahertz waves (IRMMW-THz)*, IEEE, 2016, pp. 1–2.
- [2] G Ducournau, Y Yoshimizu, S Hisatake, F Pavanello, E Peytavit, M Zaknoune, T Nagatsuma, and J. Lampin, “200 ghz coherent wireless link using photonics-based emission,” in *2014 39th International Conference on Infrared, Millimeter, and Terahertz waves (IRMMW-THz)*, IEEE, 2014, pp. 1–2.
- [3] *Flex4g-10000*, 2017. [Online]. Available: <https://bridgewave.com/flex4g-10000/>.
- [4] V. Teppati, “Millimeter-wave load-pull techniques,” 2019.
- [0] J. Su, J. Cai, X. Zheng, and L. Sun, “A robust on-wafer large signal transistor characterization method at mm-wave frequency,” *Chinese Journal of Electronics*, vol. 28, no. 4, pp. 871–877, 2019.
- [6] L. John, M. Ohlrogge, S. Wagner, C. Friesicke, A. Tessmann, A. Leuther, and T. Zwick, “In situ load-pull mmic for large-signal characterization of mhemt devices at submillimeter-wave frequencies,” in *2018 IEEE/MTT-S International Microwave Symposium-IMS*, IEEE, 2018, pp. 761–764.
- [7] D. Williams, J. Cheron, R. Chamberlin, and T. Denis, “Design of an on-chip mmwave lsna with load pull and advanced signal sources (keynote),” in *2019 93rd ARFTG Microwave Measurement Conference (ARFTG)*, IEEE, 2019, pp. 1–1.
- [8] N. Marcuvitz, *Waveguide handbook*, 21. Iet, 1951.
- [9] Q. Shen and N. S. Barker, “Distributed mems tunable matching network using minimal-contact rf-mems varactors,” *IEEE transactions on microwave theory and techniques*, vol. 54, no. 6, pp. 2646–2658, 2006.
- [10] J. R. Stanec and N. S. Barker, “A rectangular-waveguide contacting sliding short for terahertz frequency applications,” *IEEE Transactions on Microwave Theory and Techniques*, vol. 61, no. 4, pp. 1488–1495, 2013.
- [11] C. Koenen, U. Siart, T. F. Eibert, and G. D. Conway, “A self-aligning cylindrical sliding short plunger for millimeter-wave rectangular waveguides and its application in a reflection-type phase shifter,” *IEEE Transactions on Microwave Theory and Techniques*, vol. 65, no. 2, pp. 449–458, 2016.

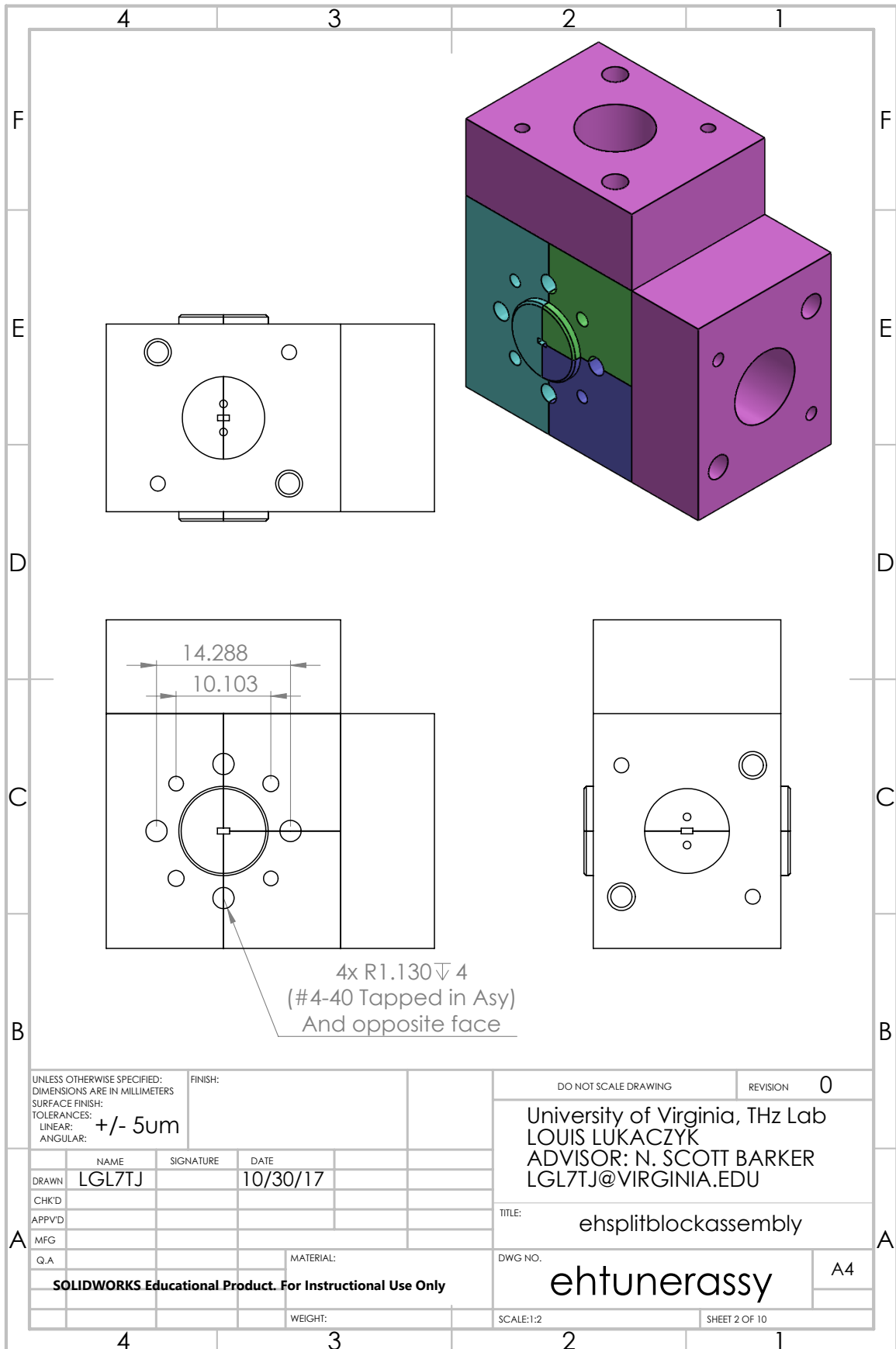
- [0] M. Pulido-Gaytán, J. Reynoso-Hernández, M. Maya-Sánchez, and J. Loo-Yau, “Calibration of a real-time load-pull system using the generalized theory of the trm technique,” in *2016 87th ARFTG Microwave Measurement Conference (ARFTG)*, IEEE, 2016, pp. 1–4.
- [0] J. Yota, H. Shen, and R. Ramanathan, “Characterization of atomic layer deposition hfo₂, al₂o₃, and plasma-enhanced chemical vapor deposition si₃n₄ as metal–insulator–metal capacitor dielectric for gaas hbt technology,” *Journal of Vacuum Science & Technology A: Vacuum, Surfaces, and Films*, vol. 31, no. 1, 01A134, 2013.
- [0] V. Teppati and C. R. Bolognesi, “Evaluation and reduction of calibration residual uncertainty in load-pull measurements at millimeter-wave frequencies,” *IEEE Transactions on Instrumentation and Measurement*, vol. 61, no. 3, pp. 817–822, 2011.

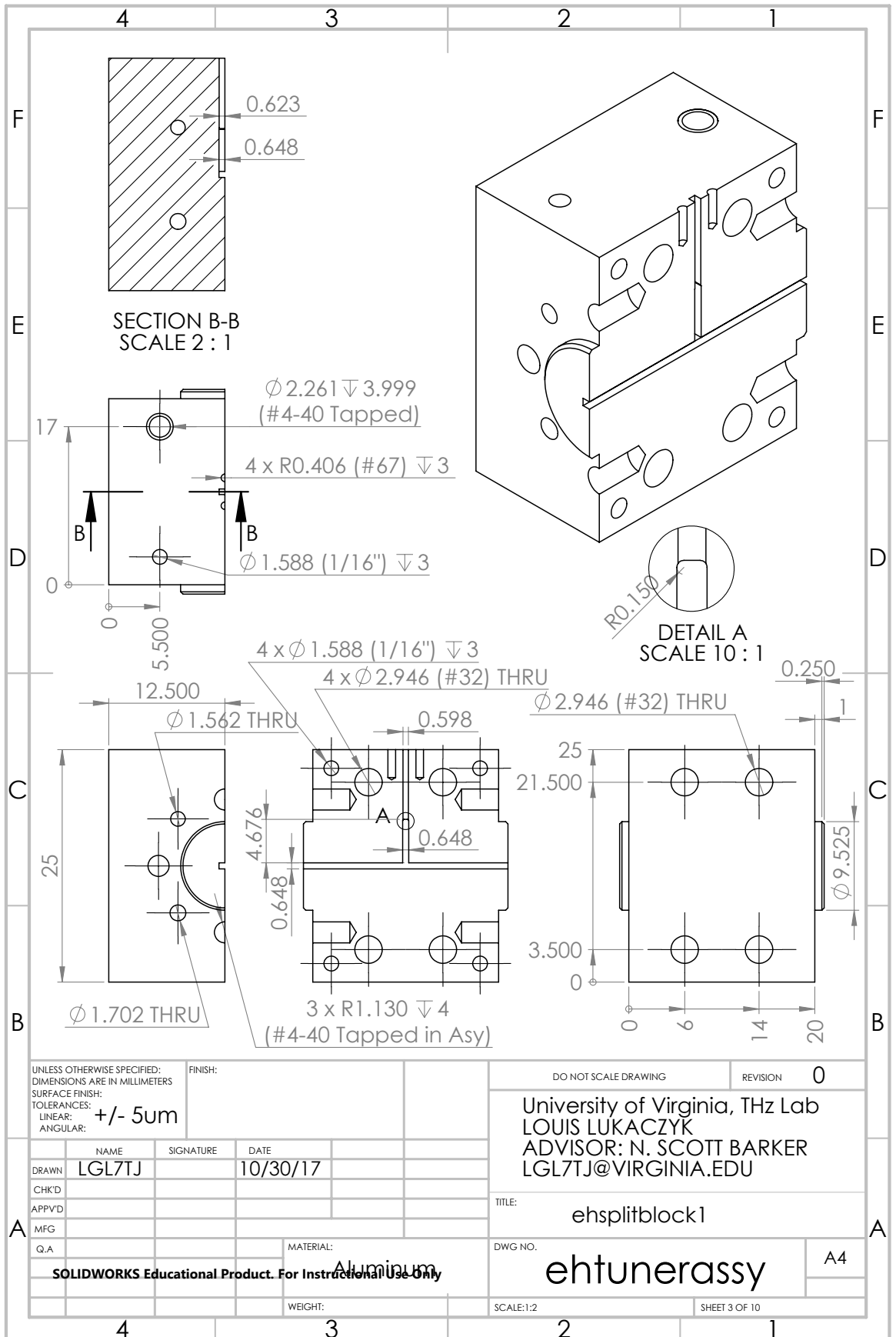
Appendix A: WR-5.1 E-H Tuner Drawings

This section shows the block drawings for the WR-5.1 E-H Tuner



UNLESS OTHERWISE SPECIFIED: DIMENSIONS ARE IN MILLIMETERS		FINISH:		DO NOT SCALE DRAWING		REVISION 0	
SURFACE FINISH:				University of Virginia, THz Lab LOUIS LUKACZYK ADVISOR: N. SCOTT BARKER LGL7TJ@VIRGINIA.EDU			
TOLERANCES:							
LINEAR: +/- 5um				TITLE: EH Assembly			
ANGULAR:				DWG NO. ehtunerassy			
DRAWN: LGL7TJ		SIGNATURE:		DATE: 10/30/17		A4	
CHKD:				SCALE: 1:2			
APPVD:				SHEET 1 OF 10			
MFG:							
Q.A:							
SOLIDWORKS Educational Product. For Instructional Use Only							
		WEIGHT:					





UNLESS OTHERWISE SPECIFIED:
 DIMENSIONS ARE IN MILLIMETERS
 SURFACE FINISH:
 TOLERANCES:
 LINEAR: +/- 5um
 ANGULAR:

FINISH:

DO NOT SCALE DRAWING

REVISION 0

University of Virginia, THz Lab
 LOUIS LUKACZYK
 ADVISOR: N. SCOTT BARKER
 LGL7TJ@VIRGINIA.EDU

NAME	SIGNATURE	DATE
DRAWN: LGL7TJ		10/30/17
CHKD:		
APPVD:		
MFG:		
Q.A:		

TITLE: ehsplitblock1

SOLIDWORKS Educational Product. For Instructional Use Only

MATERIAL: Aluminum

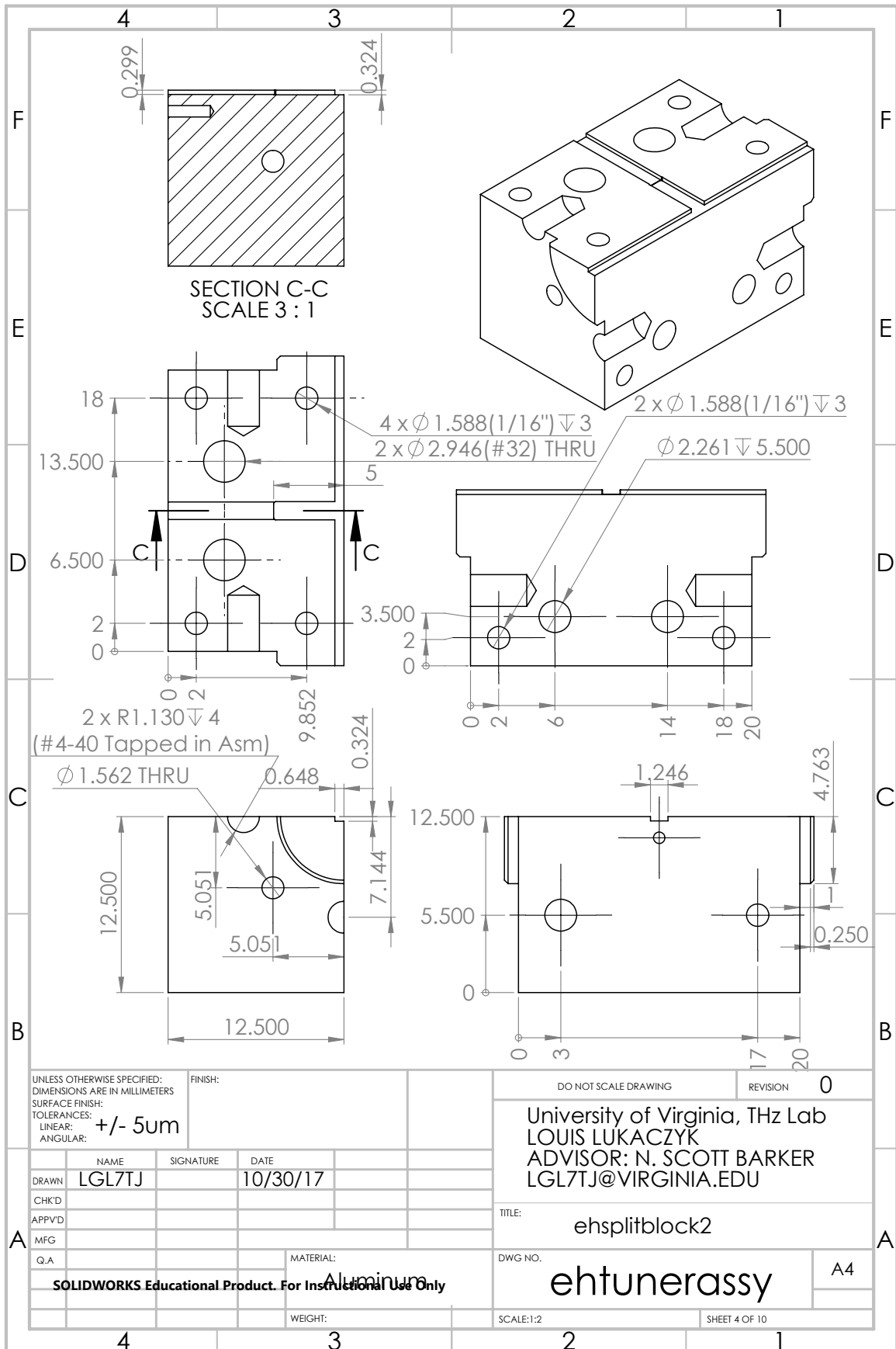
DWG NO. ehtunerassy

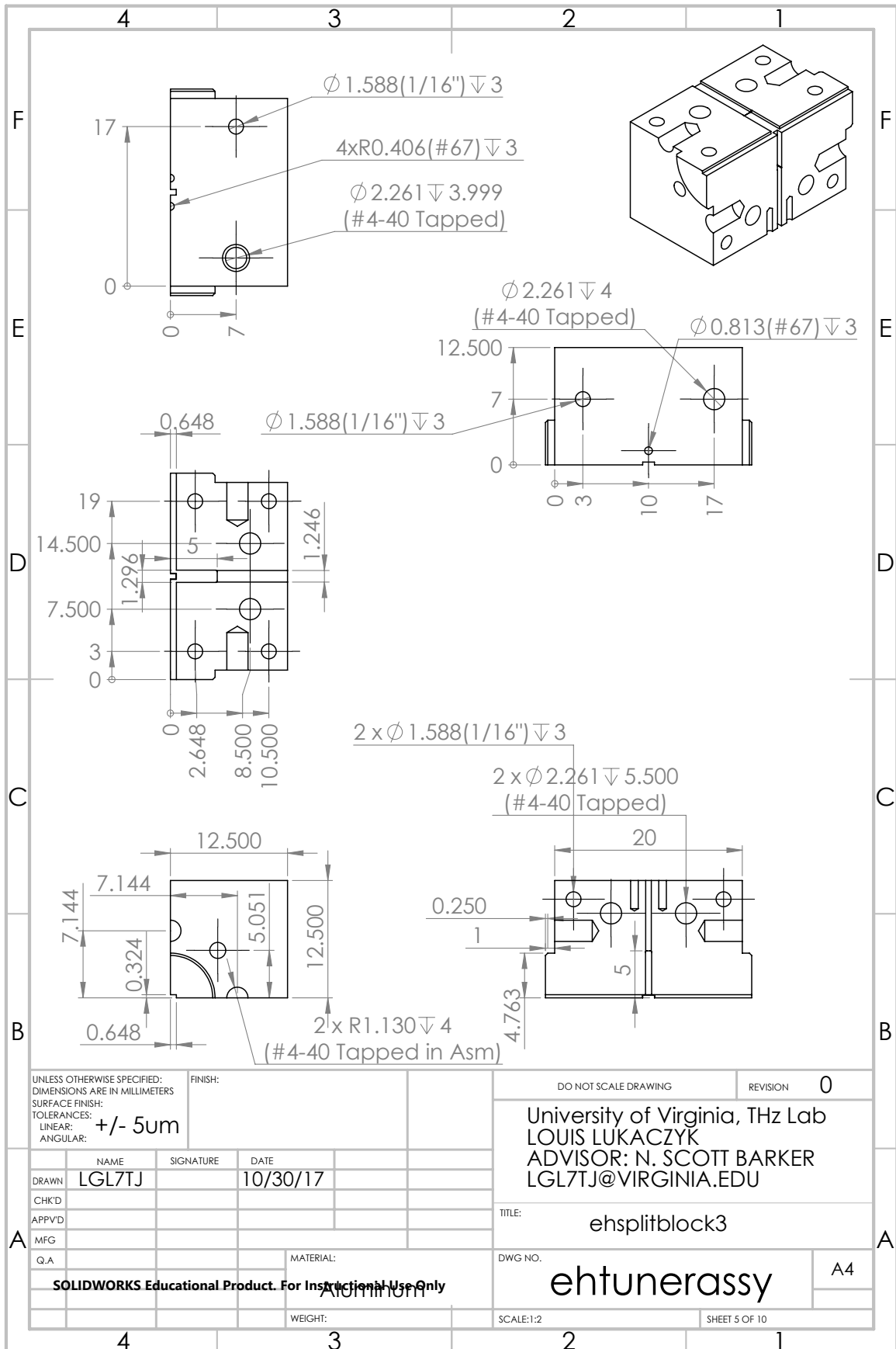
A4

WEIGHT:

SCALE: 1:2

SHEET 3 OF 10





UNLESS OTHERWISE SPECIFIED:
 DIMENSIONS ARE IN MILLIMETERS
 SURFACE FINISH:
 TOLERANCES:
 LINEAR: ± 0.5 mm
 ANGULAR:

FINISH:

DO NOT SCALE DRAWING

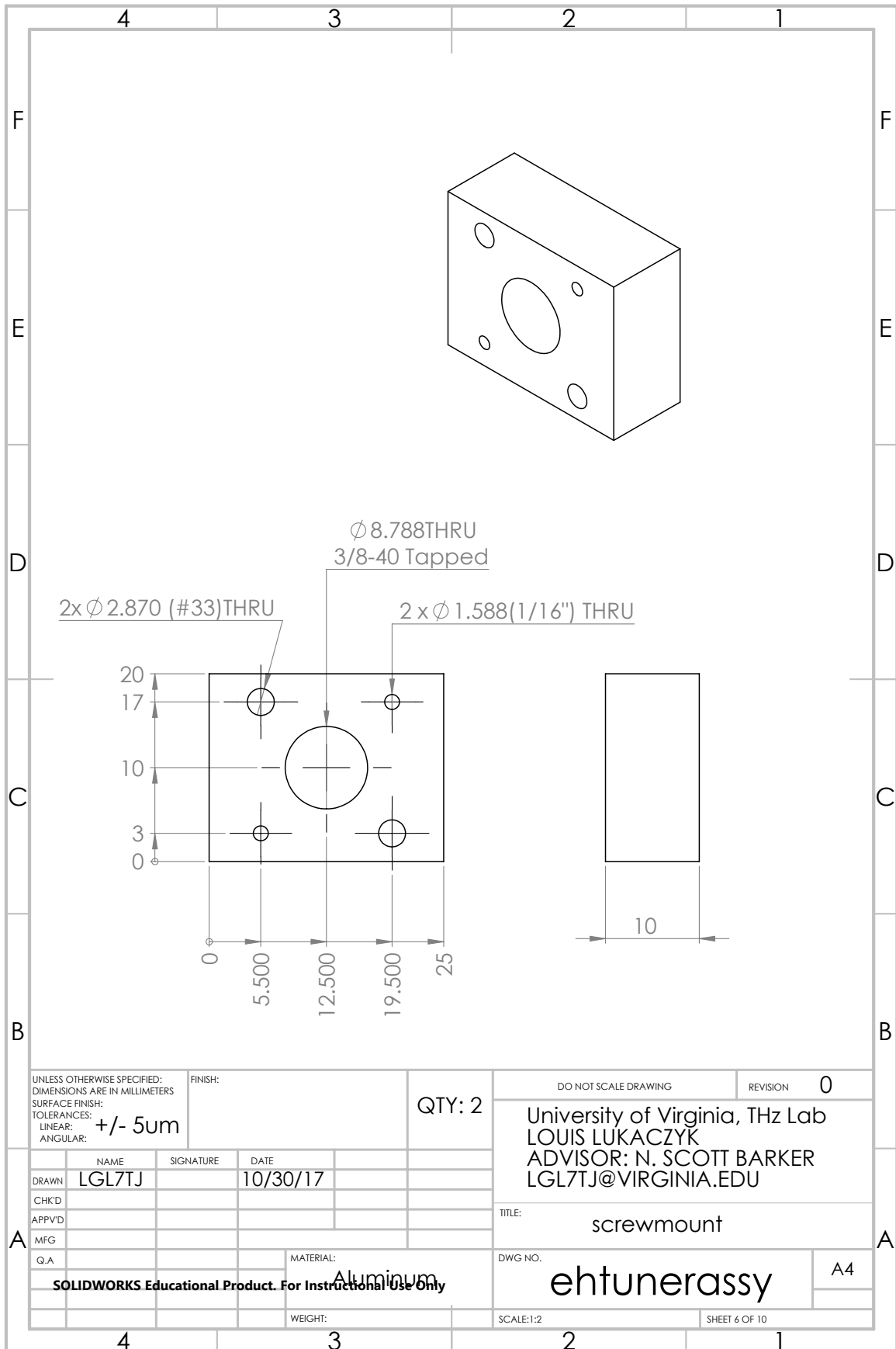
REVISION 0

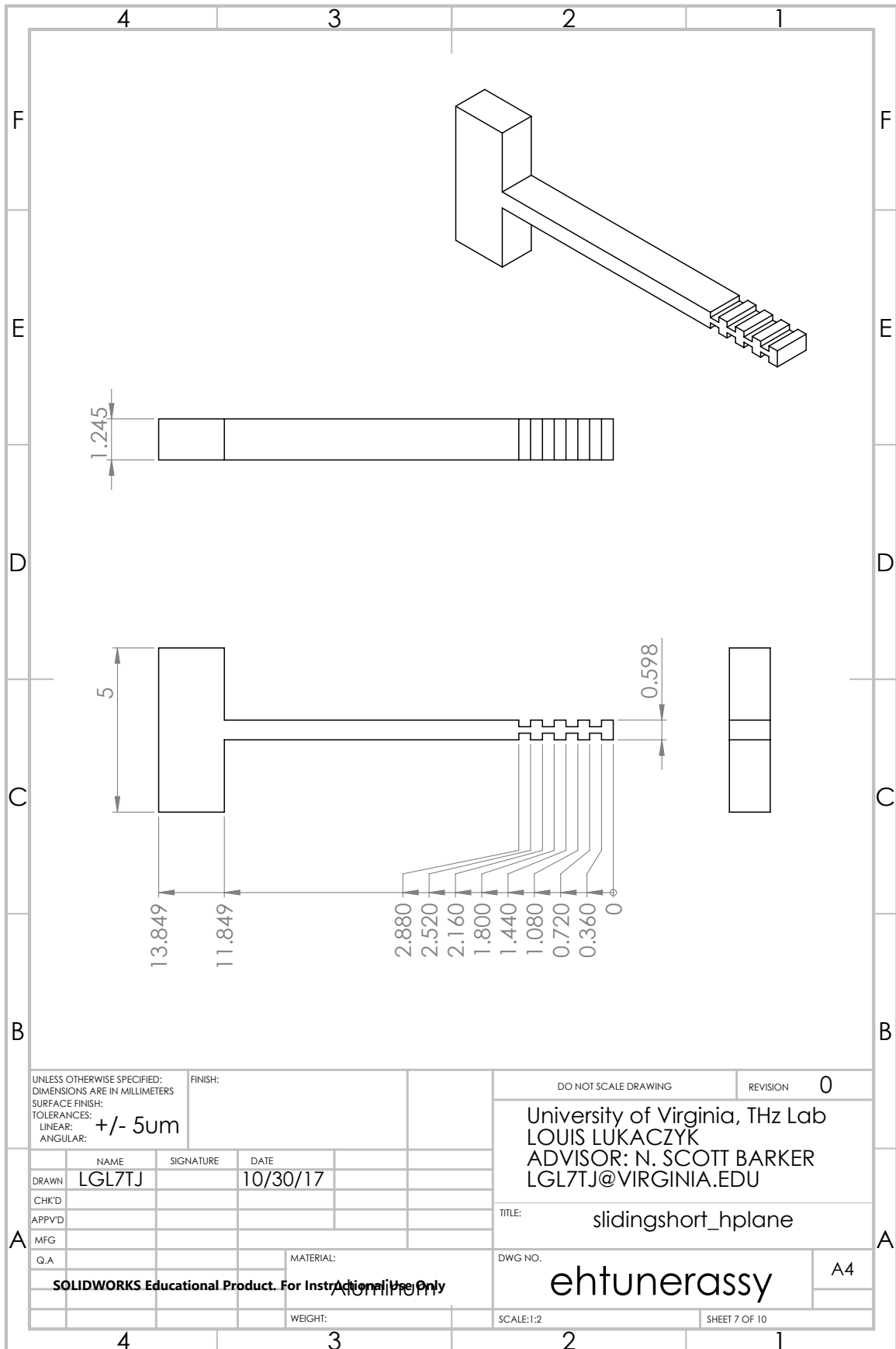
University of Virginia, THz Lab
 LOUIS LUKACZYK
 ADVISOR: N. SCOTT BARKER
 LGL7TJ@VIRGINIA.EDU

NAME	SIGNATURE	DATE
DRAWN: LGL7TJ		10/30/17
CHKD:		
APPVD:		
MFG:		
Q.A.		
MATERIAL: Aluminum		
WEIGHT:		

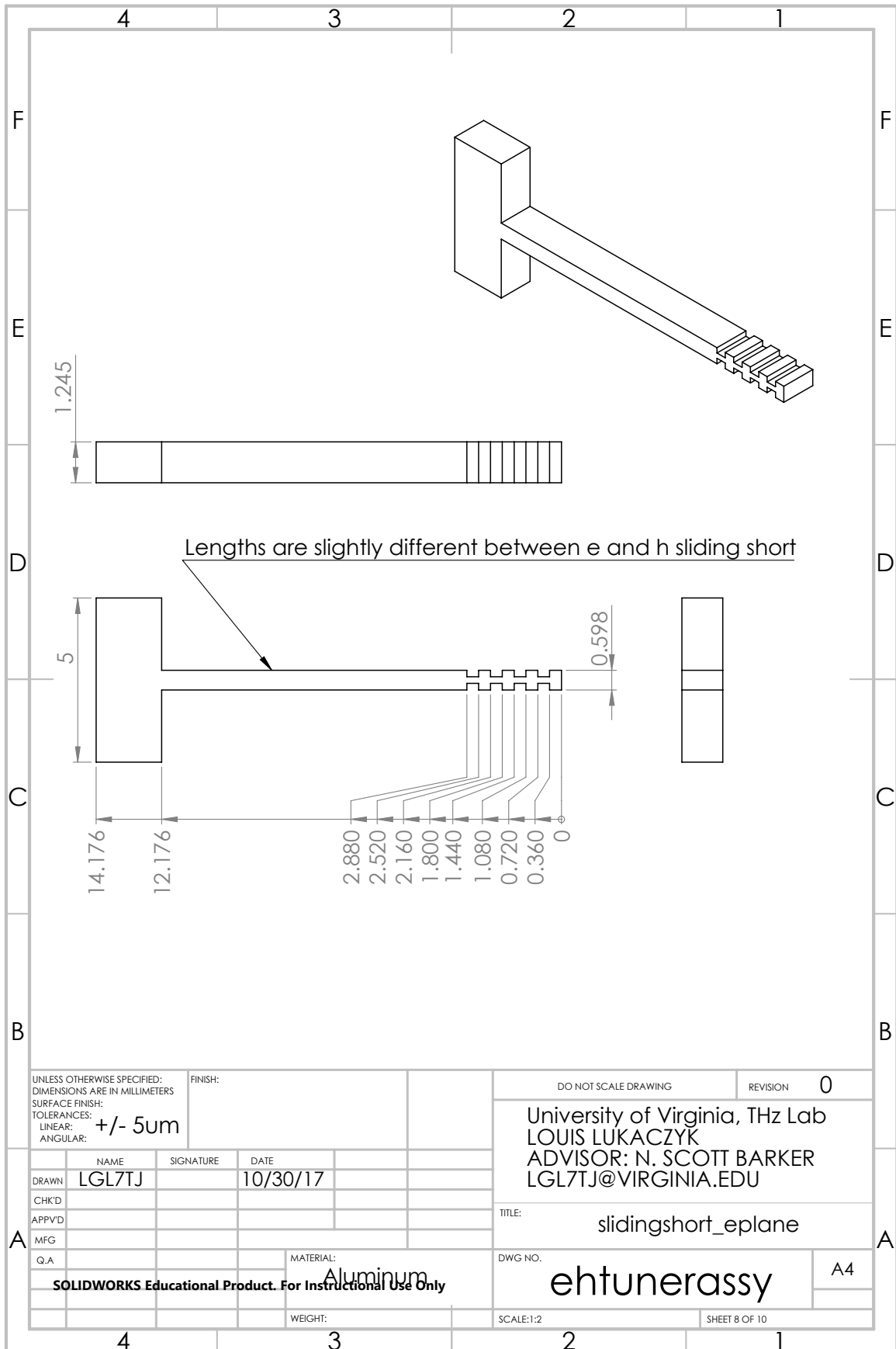
TITLE: ehsplitblock3
DWG NO. ehtunerassy
A4
SCALE: 1:2
SHEET 5 OF 10

SOLIDWORKS Educational Product. For Instructional Use Only





UNLESS OTHERWISE SPECIFIED: DIMENSIONS ARE IN MILLIMETERS		FINISH:		DO NOT SCALE DRAWING		REVISION 0	
SURFACE FINISH:				University of Virginia, THz Lab LOUIS LUKACZYK ADVISOR: N. SCOTT BARKER LGL7TJ@VIRGINIA.EDU			
TOLERANCES:							
LINEAR: +/- 5um				TITLE: slidingshort_hplane			
ANGULAR:				DWG NO. ehtunerassy			
DRAWN: LGL7TJ		SIGNATURE:		DATE: 10/30/17		A4	
CHKD:							
APPVD:							
MFG:							
Q.A:				MATERIAL:			
SOLIDWORKS Educational Product. For Instructional Use Only				WEIGHT:		SCALE: 1:2 SHEET 7 OF 10	



UNLESS OTHERWISE SPECIFIED:
 DIMENSIONS ARE IN MILLIMETERS
 SURFACE FINISH:
 TOLERANCES:
 LINEAR: +/- 5um
 ANGULAR:

FINISH:

DO NOT SCALE DRAWING

REVISION 0

University of Virginia, THz Lab
 LOUIS LUKACZYK
 ADVISOR: N. SCOTT BARKER
 LGL7TJ@VIRGINIA.EDU

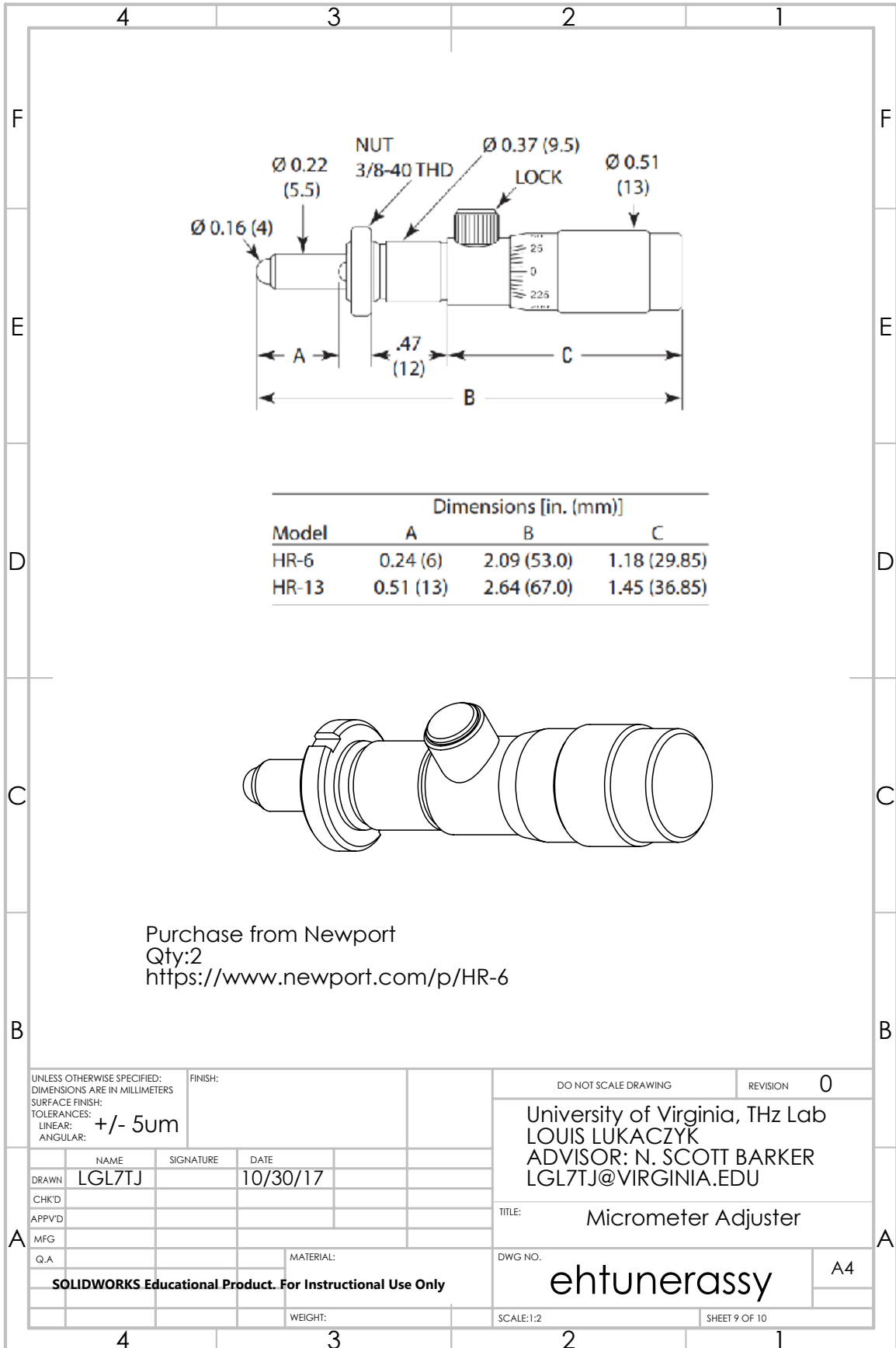
	NAME	SIGNATURE	DATE
DRAWN	LGL7TJ		10/30/17
CHKD			
APPVD			
MFG			
Q.A.			

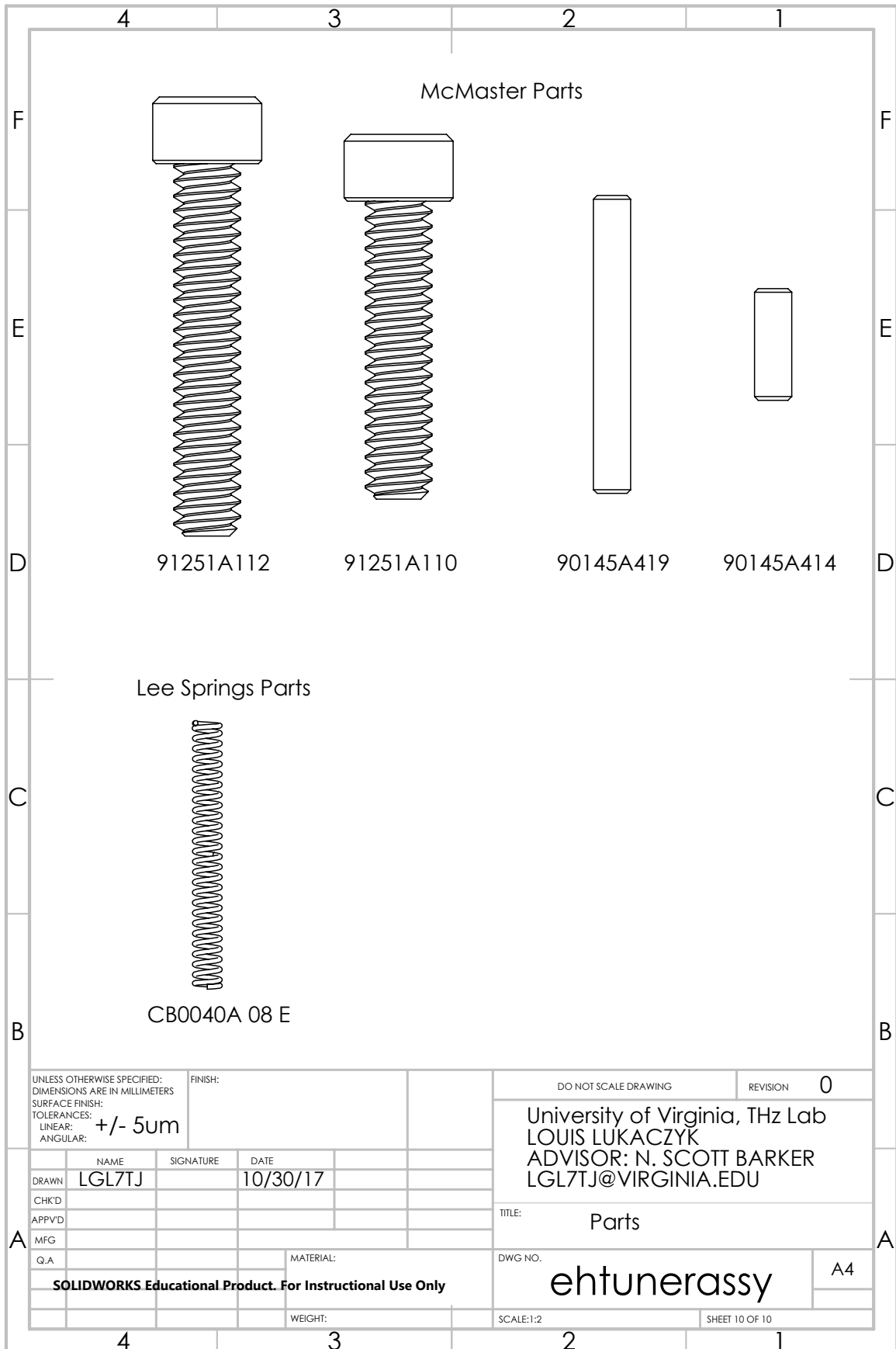
MATERIAL: Aluminum

SOLIDWORKS Educational Product. For Instructional Use Only

WEIGHT:

TITLE:	slidingshort_eplane
DWG NO.	ehtunerassy
SCALE:1:2	SHEET 8 OF 10



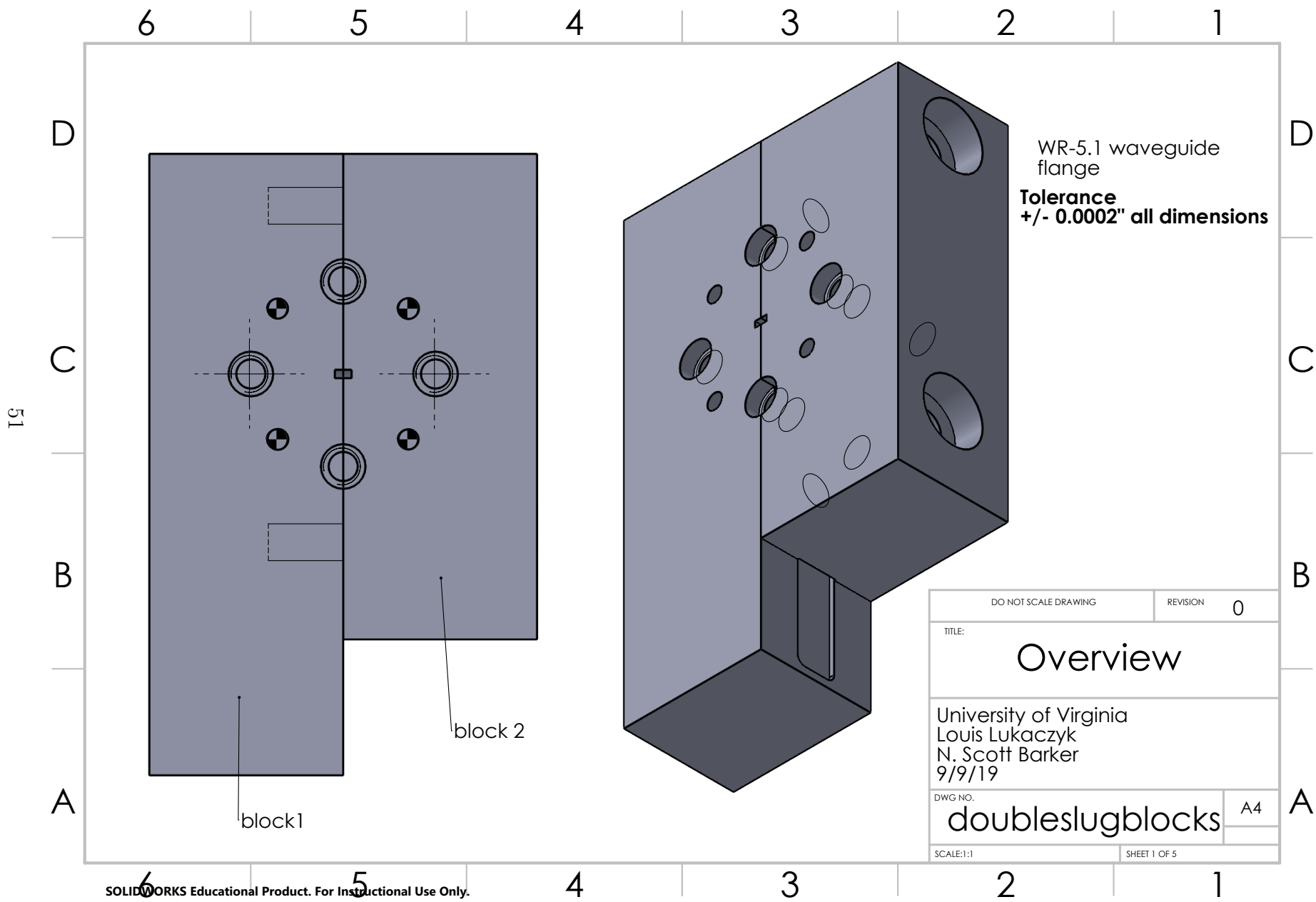


Appendix B: WR-5.1

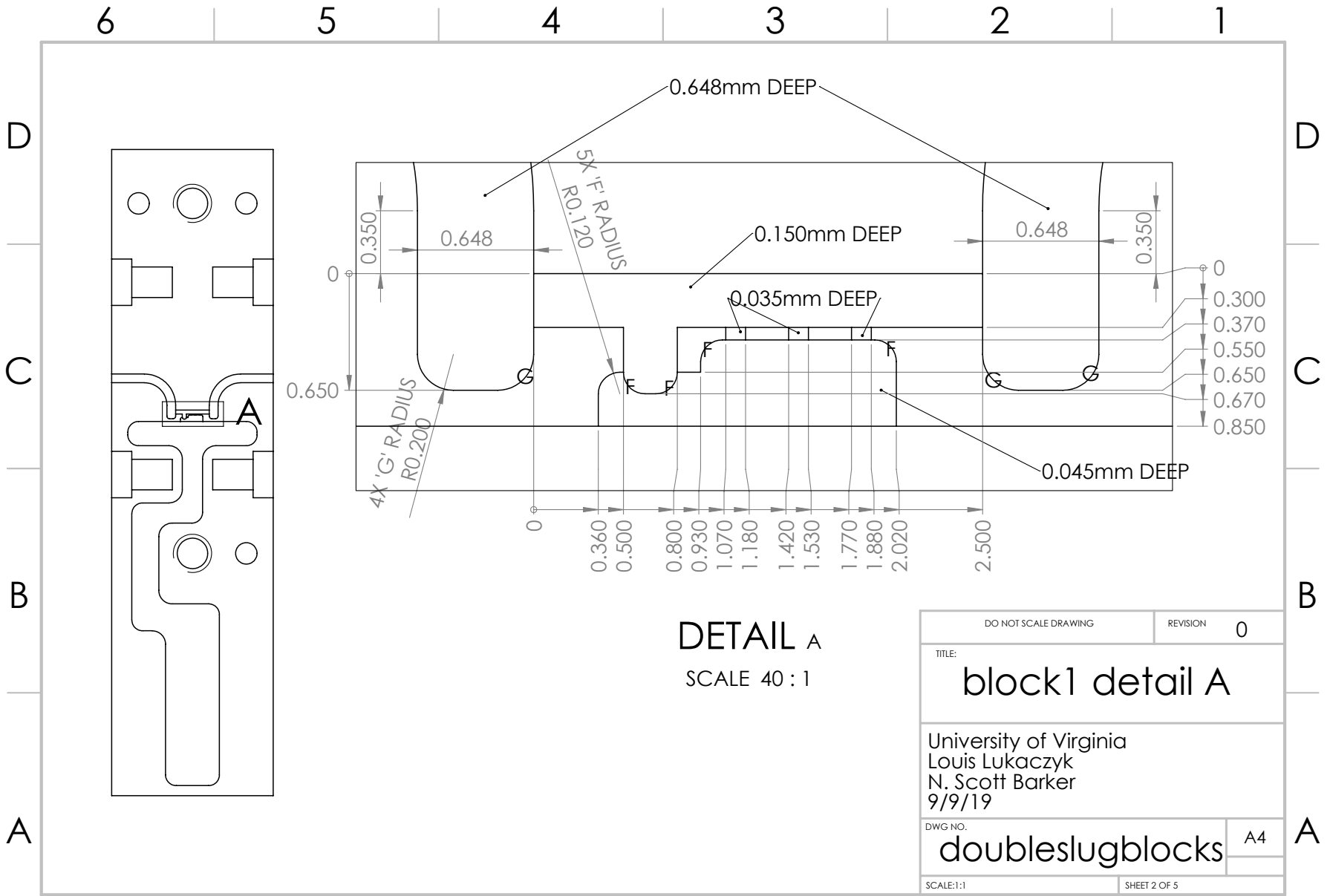
Waveguide-to-Waveguide MEMS

Double Slug Tuner Block Drawings

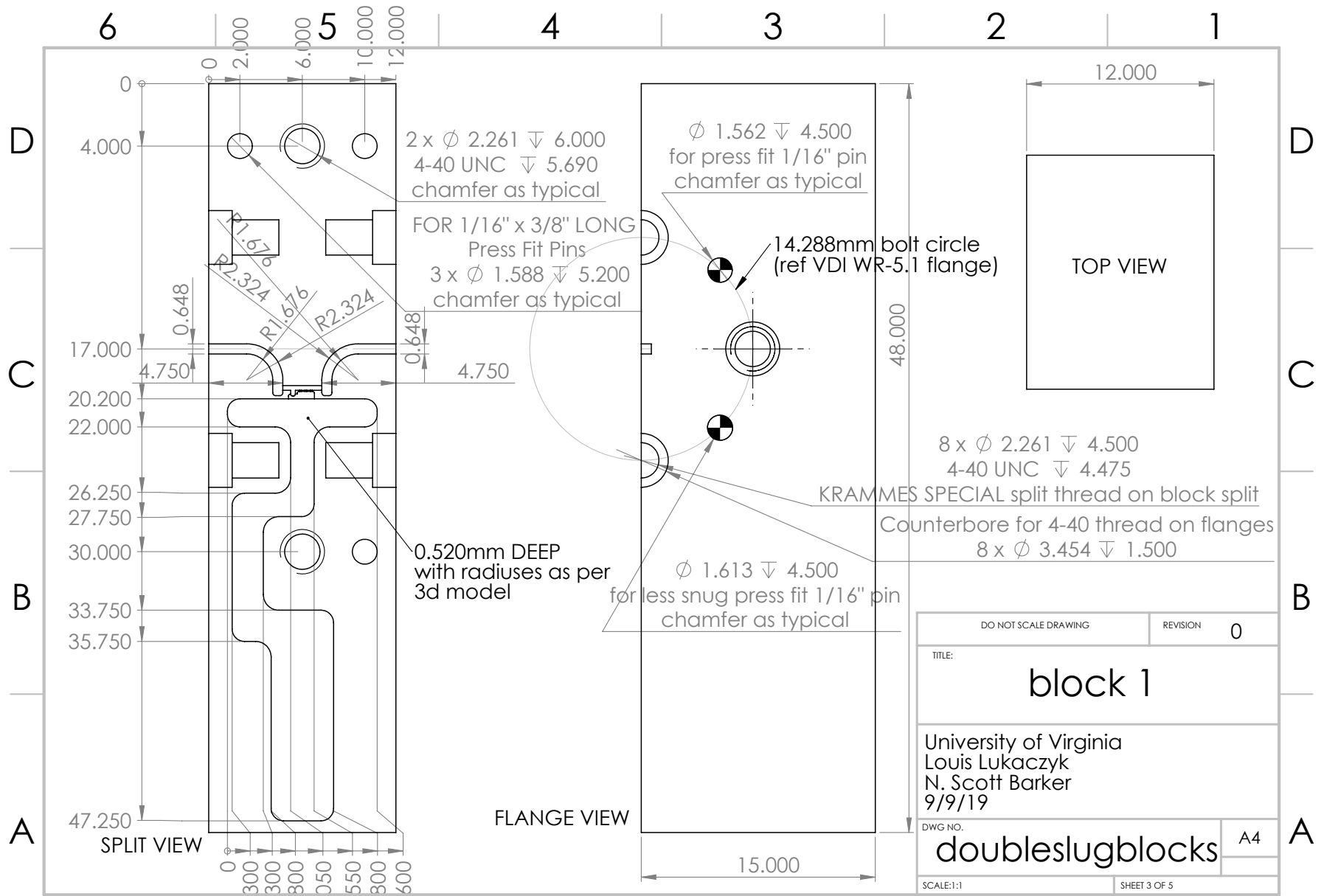
This appendix shows the block design for the proposed double slug MEMS tuner. Constructed out of aluminum or copper.



52



53



54

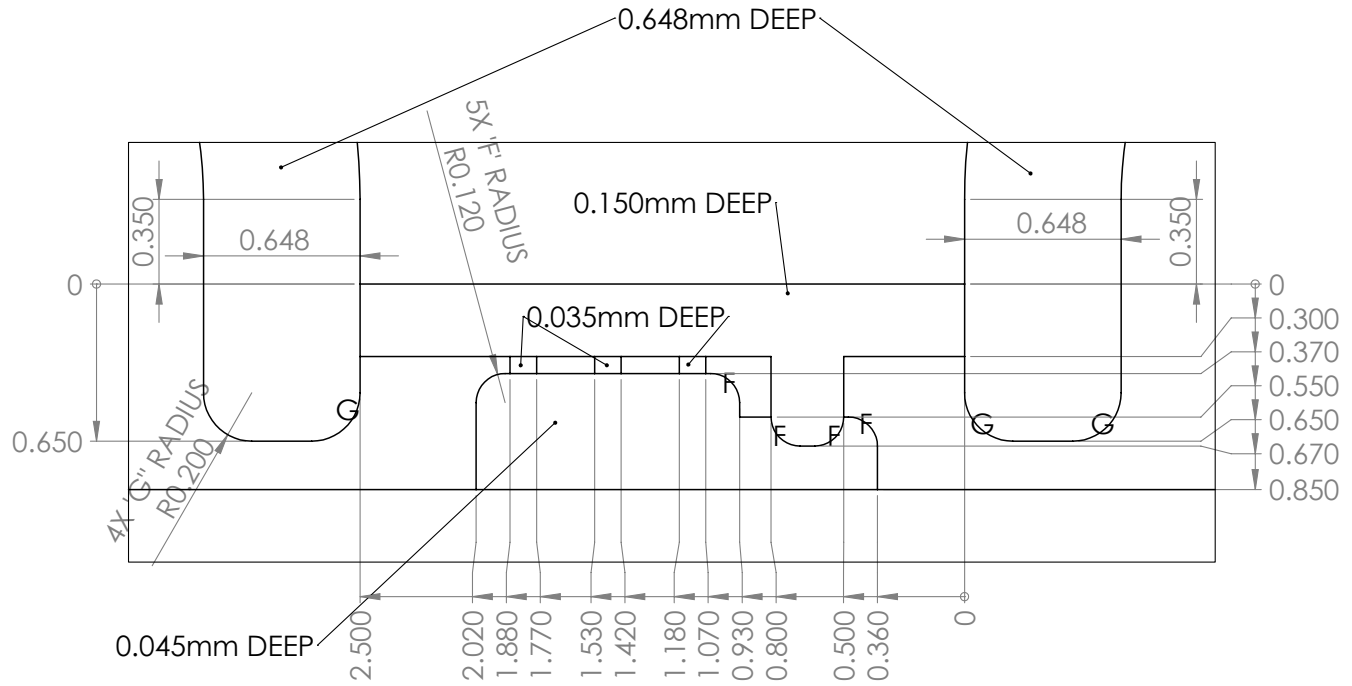
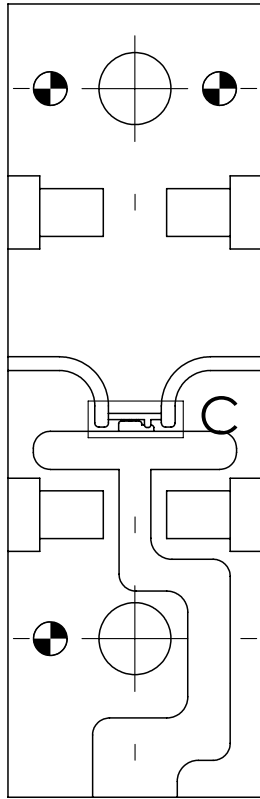
6 5 4 3 2 1

D D

C C

B B

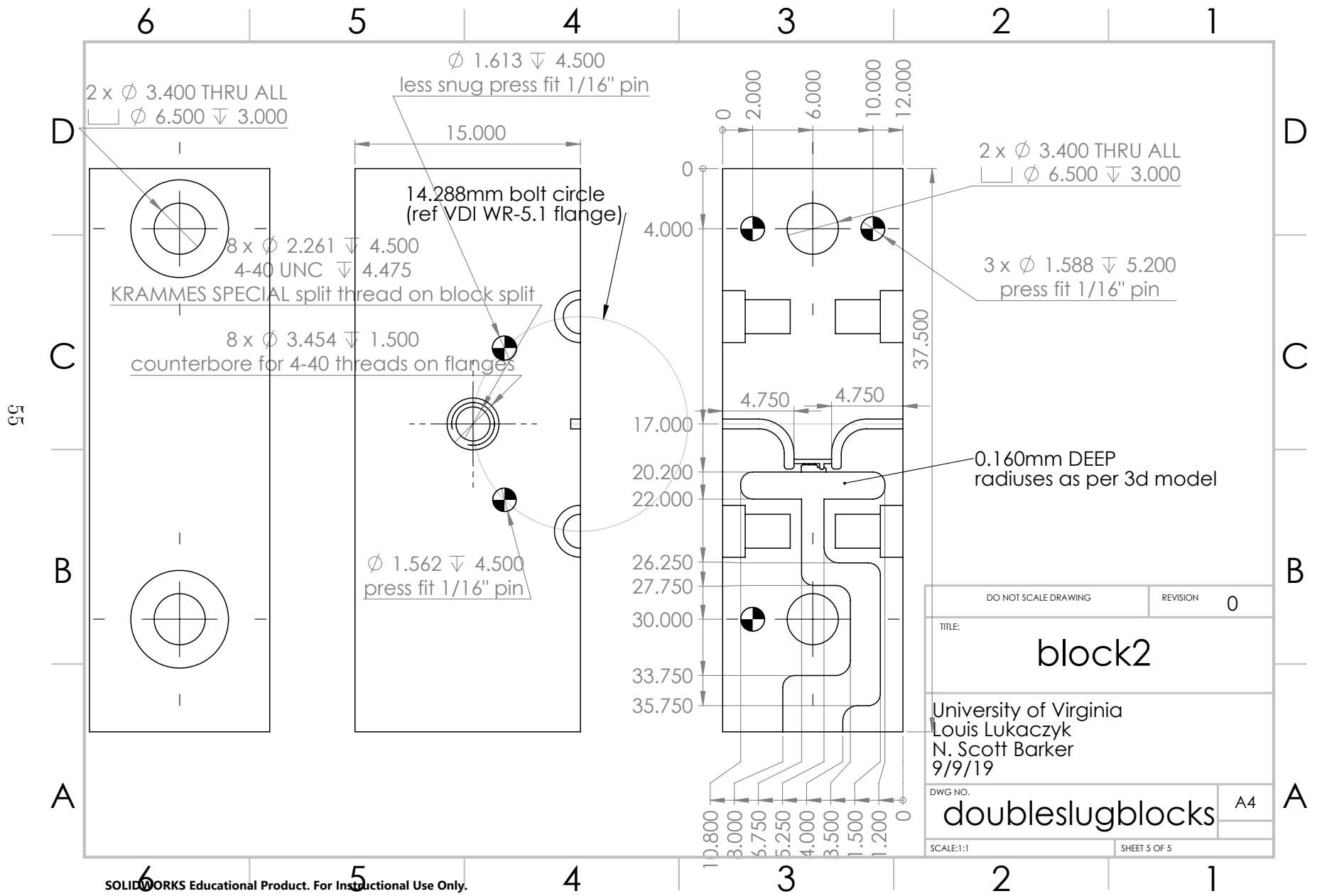
A A



DETAIL C
SCALE 40 : 1

DO NOT SCALE DRAWING	REVISION 0
TITLE: block 2 detail C	
University of Virginia Louis Lukaczyk N. Scott Barker 9/9/19	
DWG NO. doubleslugblocks	A4
SCALE:1:1	SHEET 4 OF 5

6 5 4 3 2 1



Appendix C: Python Code for Calculating Slug Sweep Simulation Settings

```
N90 = 3 # Number of section in 90 deg slug
N = 30 #total number of sections
N90up = int((N-2*N90)/3)+1 # calculate maximum number of sections in Zo
c = 1 #counter
sweeptext = 'BEGIN DSCRDATA\n'
sweeptext+='% INDEX'
for i in range(1,N+1):
    sweeptext += '\tc'+str(i)
with open('newslugbb6.dscr','a') as file1:
    for t1 in range(0,2*N90up):
        for t2 in range(0,N-2*N90-t1+1):
            sweeptext += '\n'+str(c)
            c+=1
            for swp in range(0,t1):
                sweeptext += '\t0'
            for swp in range(0,N90):
                sweeptext += '\t1'
            for swp in range(0,t2):
                sweeptext += '\t0'
            for swp in range(0,N90):
                sweeptext += '\t1'
            for swp in range(0,N-t1-t2-N90*2):
                sweeptext += '\t0'
```